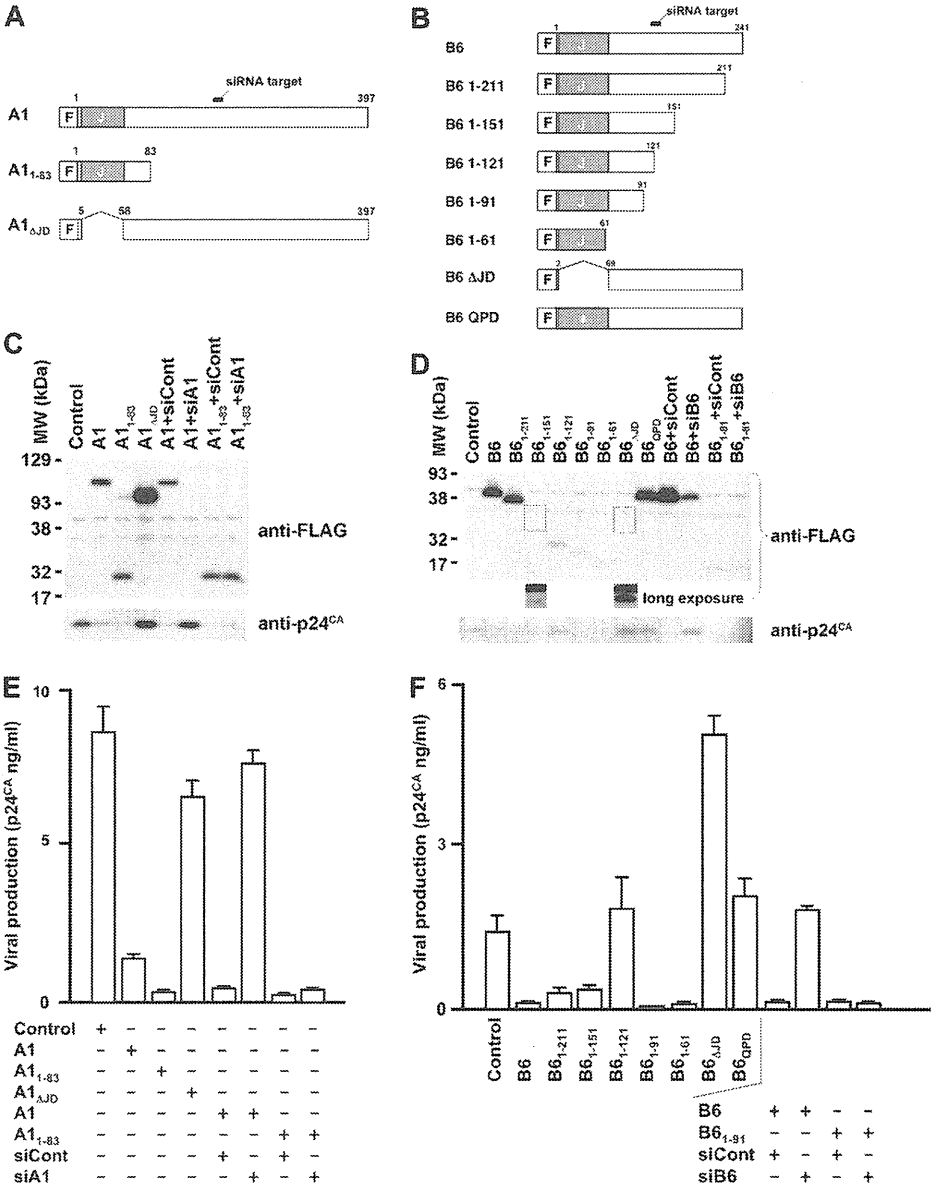

FIGURE 2. Genetic analysis of effects of HSP40A1 and B6 on inhibition of HIV-1 production. A and B, Structures of HSP40A1 (A) and B6 (B) mutants and target loci of siRNAs. C and D, Verification by Western blotting of expression of HSP40, and the effect of siRNAs against corresponding HSP40s in 293T cells. Inhibitory effects on HIV-1 production of HAP40A1 (C) and B6 (D) mutants were analyzed by immunoblotting to detect $p24^{CA}$ antigen in transfected cell lysates. E and F, Effects of HSP40 mutants on HIV-1 production. Viral production from 293T cells, transfected with proviral DNA along with expression vectors for HSP40A1 (E) or B6 (F) mutants, was measured by ELISA to detect $p24^{CA}$ antigen. Representative data from 2 or 3 independent experiments are shown.

viral transcript. Similar observations were made for Tat mRNA (data not shown).

The accumulation of HIV-1 RNA in cells is controlled by Tat and Rev, regulatory proteins encoded by HIV-1.[34] Transcription of viral gene expression is driven by a long terminal repeat (LTR) promoter, which is greatly enhanced by Tat. We investigated whether Tat-driven transcription from the LTR was affected by HSP40. To this end, Tat and HSP40 expression vectors were cotransfected into genetically engineered HeLa cells carrying an LTR-luciferase cassette (TZM-bl cells), in which the induction of luciferase represents the levels of Tat expression. Luciferase activities were not affected by any of the HSP40s (Fig. 4B), suggesting that the Tat-LTR axis is not targeted by HSP40s.

The absence of Rev results in the low steady-state accumulation of HIV-1 RNAs.[35] To investigate whether Rev function is affected by HSP40s, we compared the levels of $p24^{CA}$ expression from pCMV8.91, a CMV promoter-driven HIV-1 Gag-pol expression vector,[24] with a CMV promoter-driven human codon-optimized HIV-1 Gag-pol expression vector, psyngag-pol,[23] in a transient cotransfection assay in 293T cells. The expression of Gag-pol depends on Rev from pCMV8.91 but does not from psyngag-pol. Reduction of $p24^{CA}$ levels by HSP40s was observed when pCMV8.91 was used, consistent with the data obtained in experiments using proviral DNA (Fig. 4C, left panel, vs Fig. 1D). By contrast, such effects were not observed when psyngag-pol was used (Fig. 4C, right panel). The Gag expression from a cloned provirus of MLV lacking the functional homologue of Rev was not affected by HSP40s in the same experimental setting (data not shown). Additionally, real-time quantitative reverse transcriptase–polymerase chain reaction revealed that, when the reduction of cytoplasmic

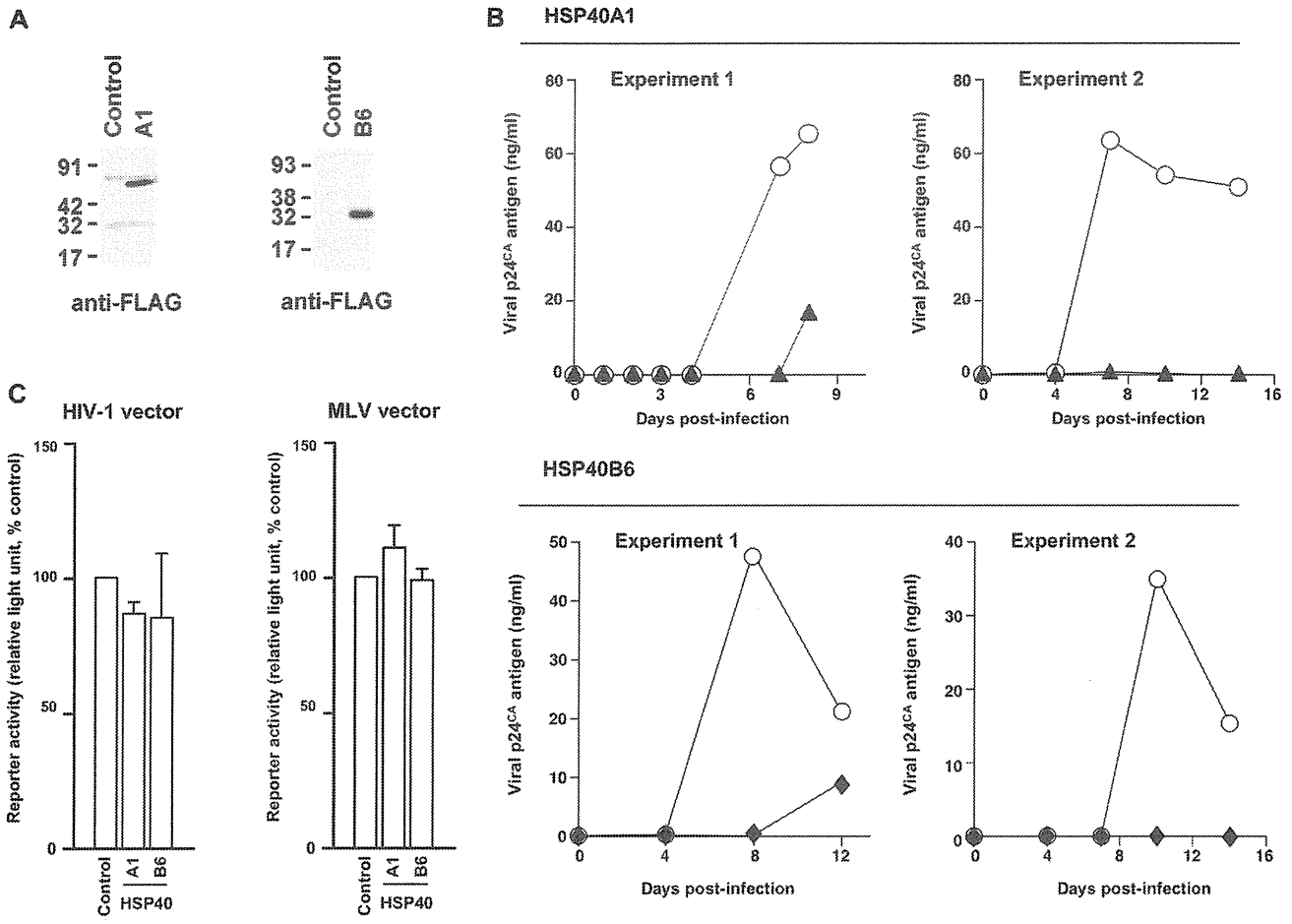

FIGURE 3. Inhibition of HIV-1 replication in T cells by HSP40A1 and B6. A, Verification by Western blotting of ectopic expression of HSP40A1 and B6 in MT-4 cells. B, Replication kinetics of HIV-1 in MT-4 cells stably expressing HSP40A1 (triangles) or HSP40B6 (diamonds). Viral replication was measured by $p24^{CA}$ antigen in the culture supernatant. Data obtained from 2 independent experiments are shown. The replication of HIV-1 in control cells is shown as circles. C, Effect of HSP40A1 and B6 expression on the entry phase of HIV-1 replication. MT-4 cells shown above were infected with VSV-G-pseudotyped MLV or HIV-1 vectors that express luciferase on infection. Representative data from 3 independent experiments are shown.

viral RNA by HSP40A1 and B6 was 24% and 20% to the control, the levels of nuclear viral RNA was 174% and 92%, respectively (data not shown). These data are consistent with the idea that Rev function is targeted by HSP40s.

Finally, we asked how HSP40s dysregulate Rev function. For Tat/LTR-driven transcription of viral genes was not affected by HSP40, we focused on the protein levels of Rev. Transient cotransfection assays were performed using Rev and HSP40 expression vectors in 293T cells. In these experiments, Rev was N-terminally tagged with an HA epitope, allowing the levels of Rev protein to evaluated by Western blot analysis using anti-HA antibody. Levels of Rev were decreased when HSP40s were coexpressed (Fig. 4D), a reduction comparable with that of $p24^{CA}$ levels under similar conditions. By contrast, expression of a control protein, mCherry-HA, was not affected by HSP40 (Fig. 4D). Similar observations were made using Rev tagged with the FLAG epitope. These results suggest that the expression of HSP40 restricts Rev expression at the posttranscriptional levels. A previously published interactome study of HIV-1 and host proteins failed to detect interactions between Rev and HSP40 family members.[36] Consistent with this, we were unable to detect a physical interaction between Rev and HSP40 by coimmunoprecipitation assay (data not shown). Additionally, both this study and previous studies failed to detect an interaction between HSP70 and Rev (data not shown; reference [36]). These data suggest that the formation of the Rev-HSP70–HSP40 complex, if it occurs at all, is transient or indirect.

DISCUSSION

In this study, we showed that the HSP70–HSP40 complex targets Rev to limit the levels of viral transcripts in cells, leading to the inhibition of viral production. Because HSP40 does not affect transcription and translation in a nonspecific manner, we speculate that the HSP70–HSP40 complex recognizes Rev specifically and inhibits the translation of Rev or

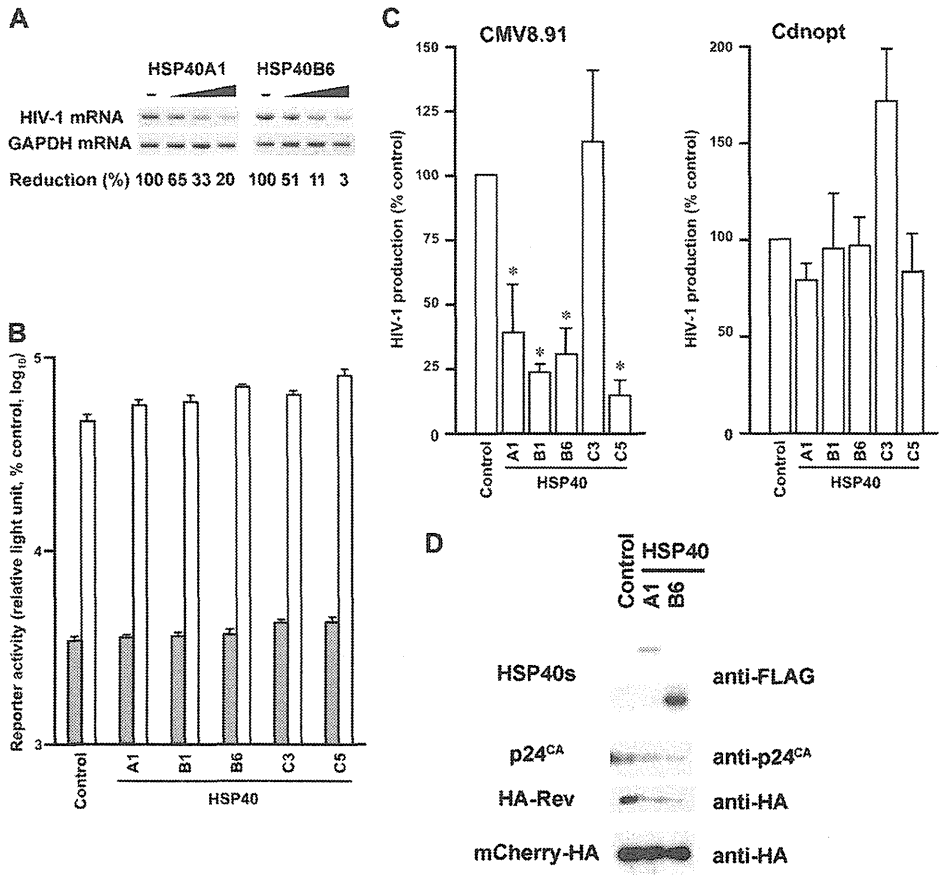

FIGURE 4. Inhibition of HIV-1 production by HSP40 at the post-transcriptional steps of the viral life cycle. A, Effect of HSP40A1 and B6 expression on levels of viral transcript. Viral transcript, represented by mRNA encoding Vpr, was detected by reverse transcriptase–polymerase chain reaction using RNA extracted from 293T cells co-transfected with proviral DNA and HSP40 expression vectors. The reductions in levels compared with the control, estimated from the band intensities, are noted below. GAPDH mRNA is shown as an internal control. Representative data from 3 independent experiments are shown. B, Effect of HSP40 on the LTR promoter-driven transcription. The promoter activity of LTR was measured by a reporter plasmid expressing luciferase. Luciferase activities in the absence (gray) and presence (white) of Tat are shown. Representative data from several independent experiments are shown. C, Effect of HSP40 on Rev-dependent or -independent gene expression. Gag expression was measured by ELISA for $p24^{CA}$ antigen. Expression vector of HSP40 members were transfected into 293T cells along with pCMV8.91, a Rev-dependent Gag expression vector that coexpressed Rev (left panel), or with psyngag-pol, a Rev-independent Gag expression vector that encoded the codon-optimized *gag-pol* gene (right panel). Asterisk indicates the statistical significance ($P < 0.01$) of each measurement to the control, determined by the Student *t* test. Representative data from 3 independent experiments are shown. D, Effect of HSP40 on expression of Rev protein. The expression vector of HA epitope tagged Rev was cotransfected with HSP40A1 or B6 expression vector into 293T cells, and protein expression was investigated by Western blot analysis. Levels of $p24^{CA}$ expression and mCherry tagged with HA epitope (controls) were investigated in parallel experiments.

accelerate its degradation. Both scenarios are counterintuitive because HSP70 chaperone activity is supposed to help proteins fold rather than degrade. The former scenario could arise due to HSP70–HSP40 complex binding to the Rev mRNA, thereby preventing its translation. The mRNA binding capacity of the HSP70–HSP40 complex has been demonstrated for Bim mRNA.[37] On the other hand, the latter scenario could arise as a result of HSP70–HSP40 complex binding to the nascent Rev protein, thereby accelerating its degradation by unknown mechanisms. We favor the former because the rate of Rev degradation was not detectably accelerated by HSP40 (data not shown). In that case, it is possible that the Rev-HSP70–HSP40 complex might be formed transiently. However, we and others have failed to convincingly detect this molecular complex, limiting the detailed functional studies. We speculate that an additional cellular factor may be necessary to link the HSP70–HSP40 complex to Rev. Alternatively, it is an open possibility that HSP40 indirectly targets Rev. These possibilities will be addressed in future studies.

Both HSP70 and HSP40 are able to bind substrates. We postulate that recognition of Rev is mediated by HSP70 because HSP40's C-terminal substrate-binding domain was dispensable for the inhibitory function of HSP40 on HIV-1 production. The HSP70 family has at least 13 members. Our preliminary data suggest that a HSP70 family member, HSPA5/BiP/Grp78, is not responsible for the observed function. It remains to be determined which HSP70 protein is the partner responsible for HSP40 inhibition of HIV-1 production.

HSP40 is expressed at lower levels than HSP70 under steady-state conditions.[32] These data imply that HSP40 is a limiting factor and explain the sensitive response of HIV-1 production to exogenously expressed HSP40. HSP40A1 and B6 mutants lacking the majority of their C-terminal portions were more potent than the full-length counterparts even expressed at low levels. These data imply that the C-terminal domain negatively regulates domain for HSP70–HSP40 complex to function. This idea is supported by the fact that $HSP40B6_{\Delta JD}$ enhanced the production of HIV-1. It is possible that $HSP40B6_{\Delta JD}$ sequesters an inhibitor of the

endogenous HSP70–HSP40 complex, freeing HSP70–HSP40 to limit HIV-1 production.

In previous studies, the HSP70–HSP40 axis has been shown to interact with HIV-1 replication.[38,39] HSP70 is incorporated into HIV-1 virions via its interaction with Gag.[38,40] However, HSP40 has not been detected in the HIV-1 virion,[40] suggesting that this observation reflects a different phenomenon from those described here. HSP40B1 has been implicated as a positive factor in HIV-1 replication.[11] However, the responsible viral factor in that study was Nef, and LTR-driven transcription was affected.[11,39] The HSP40B1-Nef axis may have a lower impact than HSP70-HSP40-Rev axis on the replication efficiency of HIV-1 in our tissue-culture models. HSP40B1 has also been implicated as a positive factor in HIV-1 replication by an siRNA-based screen.[12] On the other hand, 2 other genome-wide screens have failed to identify HSP40s as negative regulators of HIV-1 replication.[41,42] Because we did not examine all members of the HSP40 family, we cannot completely rule out possibility that one or more HSP40 proteins act on other steps of HIV-1's life cycle.

In conclusion, we have demonstrated that HSP40 family members can limit the production of HIV-1 through the activation of HSP70. Our data indicate that the HSP70–HSP40 complex has a novel antiviral function specific to HIV-1 infection. Thus, the HSP70–HSP40 complex can be considered to confer an intrinsic immunity against HIV-1. HSP40A1, B1, and B6 are expressed in T cells (our data; references [29–32]). Furthermore, HSP40B6 expression is upregulated by IFN-α,[43] and HSP40 expression is upregulated by HIV-1 infection.[39] Thus, the antiviral effect of IFN-α on HIV-1 in vivo might be partially mediated by HSP40B6.[44] Our functional cDNA library screen can complement other screens aimed at identifying regulators of HIV-1 replication.

ACKNOWLEDGMENTS

The authors thank R. Ichikawa, H. Okunaga, and K. Koyama for technical assistance.

REFERENCES

1. Fan CY, Lee S, Cyr DM, et al. Mechanisms for regulation of Hsp70 function by Hsp40. *Cell Stress Chaperones.* 2003;8:309–316.
2. Qiu XB, Shao YM, Miao S, et al. The diversity of the DnaJ/Hsp40 family, the crucial partners for Hsp70 chaperones. *Cell Mol Life Sci.* 2006;63:2560–2570.
3. Daugaard M, Rohde M, Jaattela M. The heat shock protein 70 family: highly homologous proteins with overlapping and distinct functions. *FEBS Lett.* 2007;581:3702–3710.
4. Vos MJ, Hageman J, Carra S, et al. Structural and functional diversities between members of the human HSPB, HSPH, HSPA, and DNAJ chaperone families. *Biochemistry.* 2008;47:7001–7011.
5. Sullivan CS, Pipas JM. The virus-chaperone connection. *Virology.* 2001; 287:1–8.
6. Wang RY, Huang YR, Chong KM, et al. DnaJ homolog Hdj2 facilitates Japanese encephalitis virus replication. *Virology.* 2011;8:471.
7. Sohn SY, Kim JH, Baek KW, et al. Turnover of hepatitis B virus X protein is facilitated by Hdj1, a human Hsp40/DnaJ protein. *Biochem Biophys Res Commun.* 2006;347:764–768.
8. Cheng H, Cenciarelli C, Tao M, et al. HTLV-1 Tax-associated hTid-1, a human DnaJ protein, is a repressor of Ikappa B kinase beta subunit. *J Biol Chem.* 2002;277:20605–20610.
9. Glotzer JB, Saltik M, Chiocca S, et al. Activation of heat-shock response by an adenovirus is essential for virus replication. *Nature.* 2000;407:207–211.
10. Eom CY, Lehman IR. The human DnaJ protein, hTid-1, enhances binding of a multimer of the herpes simplex virus type 1 UL9 protein to oris, an origin of viral DNA replication. *Proc Natl Acad Sci U S A.* 2002;99: 1894–1898.
11. Kumar M, Mitra D. Heat shock protein 40 is necessary for human immunodeficiency virus-1 Nef-mediated enhancement of viral gene expression and replication. *J Biol Chem.* 2005;280:40041–40050.
12. Brass AL, Dykxhoorn DM, Benita Y, et al. Identification of host proteins required for HIV infection through a functional genomic screen. *Science.* 2008;319:921–926.
13. Cheng X, Belshan M, Ratner L. Hsp40 facilitates nuclear import of the human immunodeficiency virus type 2 Vpx-mediated preintegration complex. *J Virol.* 2008;82:1229–1237.
14. Goodwin EC, Lipovsky A, Inoue T, et al. BiP and multiple DNAJ molecular chaperones in the endoplasmic reticulum are required for efficient simian virus 40 infection. *MBio.* 2011;2:e00101–e00111. doi: 00110.01128/mBio.00101-00111.
15. Melville MW, Tan SL, Wambach M, et al. The cellular inhibitor of the PKR protein kinase, P58(IPK), is an influenza virus-activated co-chaperone that modulates heat shock protein 70 activity. *J Biol Chem.* 1999;274: 3797–3803.
16. Yi Z, Sperzel L, Nurnberger C, et al. Identification and characterization of the host protein DNAJC14 as a broadly active flavivirus replication modulator. *PLoS Pathog.* 2011;7:e1001255.
17. Pipas JM. Molecular chaperone function of the SV40 large T antigen. *Dev Biol Stand.* 1998;94:313–319.
18. Urano E, Kariya Y, Futahashi Y, et al. Identification of the P-TEFb complex-interacting domain of Brd4 as an inhibitor of HIV-1 replication by functional cDNA library screening in MT-4 cells. *FEBS Lett.* 2008; 582:4053–4058.
19. Urano E, Ichikawa R, Morikawa Y, et al. T cell-based functional cDNA library screening identified SEC14-like 1a carboxy-terminal domain as a negative regulator of human immunodeficiency virus replication. *Vaccine.* 2010;28(suppl 2):B68–B74.
20. Watanabe T, Urano E, Miyauchi K, et al. The hematopoietic cell-specific Rho GTPase inhibitor ARHGDIB/D4GDI limits HIV type 1 replication. *AIDS Res Hum Retroviruses.* 2012;28:913–922.
21. Kameoka M, Kitagawa Y, Utachee P, et al. Identification of the suppressive factors for human immunodeficiency virus type-1 replication using the siRNA mini-library directed against host cellular genes. *Biochem Biophys Res Commun.* 2007;359:729–734.
22. Komano J, Miyauchi K, Matsuda Z, et al. Inhibiting the Arp2/3 complex limits infection of both intracellular mature vaccinia virus and primate lentiviruses. *Mol Biol Cell.* 2004;15:5197–5207.
23. Wagner R, Graf M, Bieler K, et al. Rev-independent expression of synthetic gag-pol genes of human immunodeficiency virus type 1 and simian immunodeficiency virus: implications for the safety of lentiviral vectors. *Hum Gene Ther.* 2000;11:2403–2413.
24. Zufferey R, Nagy D, Mandel RJ, et al. Multiply attenuated lentiviral vector achieves efficient gene delivery in vivo. *Nat Biotechnol.* 1997; 15:871–875.
25. Urano E, Kuramochi N, Ichikawa R, et al. Novel postentry inhibitor of human immunodeficiency virus type 1 replication screened by yeast membrane-associated two-hybrid system. *Antimicrob Agents Chemother.* 2011;55:4251–4260.
26. Shimizu S, Urano E, Futahashi Y, et al. Inhibiting lentiviral replication by HEXIM1, a cellular negative regulator of the CDK9/cyclin T complex. *AIDS.* 2007;21:575–582.
27. Urano E, Shimizu S, Futahashi Y, et al. Cyclin K/CPR4 inhibits primate lentiviral replication by inactivating Tat/positive transcription elongation factor b-dependent long terminal repeat transcription. *AIDS.* 2008;22: 1081–1083.
28. Urano E, Aoki T, Futahashi Y, et al. Substitution of the myristoylation signal of human immunodeficiency virus type 1 Pr55Gag with the phospholipase C-delta1 pleckstrin homology domain results in infectious pseudovirion production. *J Gen Virol.* 2008;89(pt 12):3144–3149.
29. Cheng H, Cenciarelli C, Shao Z, et al. Human T cell leukemia virus type 1 Tax associates with a molecular chaperone complex containing hTid-1 and Hsp70. *Curr Biol.* 2001;11:1771–1775.

30. Lo JF, Zhou H, Fearns C, et al. Tid1 is required for T cell transition from double-negative 3 to double-positive stages. *J Immunol.* 2005;174:6105–6112.
31. Zhang Y, Yang Z, Cao Y, et al. The Hsp40 family chaperone protein DnaJB6 enhances Schlafen1 nuclear localization which is critical for promotion of cell-cycle arrest in T-cells. *Biochem J.* 2008;413:239–250.
32. Kolker E, Higdon R, Haynes W, et al. MOPED: Model Organism Protein Expression Database. *Nucleic Acids Res.* 2012;40(database issue): D1093–D1099.
33. Qian YQ, Patel D, Hartl FU, et al. Nuclear magnetic resonance solution structure of the human Hsp40 (HDJ-1) J-domain. *J Mol Biol.* 1996;260: 224–235.
34. Bolinger C, Boris-Lawrie K. Mechanisms employed by retroviruses to exploit host factors for translational control of a complicated proteome. *Retrovirology.* 2009;6:8.
35. Schwartz S, Felber BK, Pavlakis GN. Distinct RNA sequences in the gag region of human immunodeficiency virus type 1 decrease RNA stability and inhibit expression in the absence of Rev protein. *J Virol.* 1992;66:150–159.
36. Jager S, Cimermancic P, Gulbahce N, et al. Global landscape of HIV-human protein complexes. *Nature.* 2012;481:365–370. doi: 310.1038/nature10719.
37. Matsui H, Asou H, Inaba T. Cytokines direct the regulation of Bim mRNA stability by heat-shock cognate protein 70. *Mol Cell.* 2007;25:99–112.
38. Agostini I, Popov S, Li J, et al. Heat-shock protein 70 can replace viral protein R of HIV-1 during nuclear import of the viral preintegration complex. *Exp Cell Res.* 2000;259:398–403.
39. Kumar M, Rawat P, Khan SZ, et al. Reciprocal regulation of human immunodeficiency virus-1 gene expression and replication by heat shock proteins 40 and 70. *J Biol.* 2011;410:944–958.
40. Ott DE. Cellular proteins detected in HIV-1. *Rev Med Virol.* 2008;18: 159–175.
41. Konig R, Zhou Y, Elleder D, et al. Global analysis of host-pathogen interactions that regulate early-stage HIV-1 replication. *Cell.* 2008;135: 49–60.
42. Zhou H, Xu M, Huang Q, et al. Genome-scale RNAi screen for host factors required for HIV replication. *Cell Host Microbe. 2008*;4:495–504.
43. Ji X, Cheung R, Cooper S, Li Q, et al. Interferon alfa regulated gene expression in patients initiating interferon treatment for chronic hepatitis C. *Hepatology.* 2003;37:610–621.
44. Shirazi Y, Pitha PM. Alpha interferon inhibits early stages of the human immunodeficiency virus type 1 replication cycle. *J Virol.* 1992;66:1321–1328.

Human CD1c$^+$ Myeloid Dendritic Cells Acquire a High Level of Retinoic Acid–Producing Capacity in Response to Vitamin D_3

Takayuki Sato,*,† Toshio Kitawaki,* Haruyuki Fujita,* Makoto Iwata,†,‡ Tomonori Iyoda,†,§ Kayo Inaba,†,§ Toshiaki Ohteki,†,¶ Suguru Hasegawa,‖ Kenji Kawada,‖ Yoshiharu Sakai,‖ Hiroki Ikeuchi,# Hiroshi Nakase,** Akira Niwa,††,‡‡ Akifumi Takaori-Kondo,* and Norimitsu Kadowaki*,†

All-*trans*-retinoic acid (RA) plays a critical role in maintaining immune homeostasis. Mouse intestinal CD103$^+$ dendritic cells (DCs) produce a high level of RA by highly expressing retinal dehydrogenase (RALDH)2, an enzyme that converts retinal to RA, and induce gut-homing T cells. However, it has not been identified which subset of human DCs produce a high level of RA. In this study, we show that CD1c$^+$ blood myeloid DCs (mDCs) but not CD141^{high} mDCs or plasmacytoid DCs exhibited a high level of RALDH2 mRNA and aldehyde dehydrogenase (ALDH) activity in an RA- and p38-dependent manner when stimulated with 1α,25-dihydroxyvitamin D_3 (VD_3) in the presence of GM-CSF. The ALDH activity was abrogated by TLR ligands or TNF. CD103$^-$ rather than CD103$^+$ human mesenteric lymph node mDCs gained ALDH activity in response to VD_3. Furthermore, unlike in humans, mouse conventional DCs in the spleen and mesenteric lymph nodes gained ALDH activity in response to GM-CSF alone. RALDH2^{high} CD1c$^+$ mDCs stimulated naive CD4$^+$ T cells to express gut-homing molecules and to produce Th2 cytokines in an RA-dependent manner. This study suggests that CD1c$^+$ mDCs are a major human DC subset that produces RA in response to VD_3 in the steady state. The "vitamin D – CD1c$^+$ mDC – RA" axis may constitute an important immune component for maintaining tissue homeostasis in humans. *The Journal of Immunology*, **2013, 191: 3152–3160.**

Dendritic cells (DCs) play a pivotal role in controlling immune responses in terms of their magnitude and quality, such as immunity versus tolerance, depending on the tissue milieu. This eventually leads to maintaining immune homeostasis by eliminating pathogens and by avoiding harmful inflammation. Recent studies using mice revealed the importance of all-*trans*-retinoic acid (hereafter referred to as RA) derived from DCs in maintaining immune homeostasis in the intestine (1) and possibly in other organs (2). It has been shown that CD103$^+$ DCs in lamina propria and mesenteric lymph nodes (MLNs) produce RA and thus to promote the generation of gut-homing regulatory T (Treg) cells (3). GM-CSF (4) and RA (4–8) are pivotal factors to induce mouse DCs to express retinal dehydrogenase (RALDH)2, which is encoded by the aldehyde dehydrogenase 1 family, member A2 (*ALDH1A2*) gene and converts retinal to RA. IL-4 (4, 9) and TLR ligands (2, 4, 5, 10–12) augment the expression of RALDH2. These studies have presented a model that appropriately stimulated CD103$^+$ DCs in gut-associated tissues produce RA and thus induce gut-homing Treg cells, resulting in maintaining immune homeostasis in the intestine in mice. Surprisingly, however, human DCs that express a high level of RALDH have not been identified.

Human DC subsets in blood and lymphoid tissues are composed of myeloid DCs (mDCs) and plasmacytoid DCs (pDCs) (13). mDCs are further subdivided into CD141 (BDCA-3)^{high} mDCs and CD1c (BDCA-1)$^+$ mDCs, and the former corresponds to mouse CD8$^+$ CD11b$^-$ conventional DCs (cDCs) in lymphoid tissues (14–16) and CD103$^+$ cDCs in nonlymphoid tissues (17) that efficiently cross-present Ags. In contrast, distinctive functions of the latter, which is likely equivalent to mouse CD8$^-$CD11b$^+$ cDCs (18), have been elusive. In addition, monocytes and CD34$^+$ hematopoietic progenitors can differentiate into DCs in the presence of appropriate cytokine mixtures. However, it remains unclear which DCs in situ correspond to DCs induced in vitro from monocytes or CD34$^+$ progenitors. Therefore, it is important to obtain data using DCs isolated from blood and tissues to gain an insight into physiological and clinical relevance of basic researches on human DCs.

*Department of Hematology and Oncology, Graduate School of Medicine, Kyoto University, Kyoto 606-8507, Japan; †Japan Science and Technology Agency, Core Research for Evolutional Science and Technology, Tokyo 102-0076, Japan; ‡Laboratory of Immunology, Kagawa School of Pharmaceutical Sciences, Tokushima Bunri University, Kagawa 769-2193, Japan; §Division of Systemic Life Science, Department of Animal Development and Physiology, Laboratory of Immunology, Graduate School of Biostudies, Kyoto University, Kyoto 606-8501, Japan; ¶Department of Biodefense Research, Medical Research Institute, Tokyo Medical and Dental University, Tokyo 101-0062, Japan; ‖Department of Surgery, Graduate School of Medicine, Kyoto University, Kyoto 606-8507, Japan; #Department of Surgery, Hyogo College of Medicine, Hyogo 663-8501, Japan; **Department of Gastroenterology and Hepatology, Graduate School of Medicine, Kyoto University, Kyoto 606-8507, Japan; ††Department of Pediatrics, Graduate School of Medicine, Kyoto University, Kyoto 606-8507, Japan; and ‡‡Department of Clinical Application, Center for iPS Cell Research and Application, Kyoto University, Kyoto 606-8507, Japan

Received for publication December 26, 2012. Accepted for publication July 16, 2013.

This work was supported by research funding from the Japan Science and Technology Agency, Core Research for Evolutional Science and Technology (to N.K.).

Address correspondence and reprint requests to Dr. Norimitsu Kadowaki, Department of Hematology and Oncology, Graduate School of Medicine, Kyoto University, 54 Shogoin Kawahara-cho, Sakyo-ku, Kyoto 606-8507, Japan. E-mail address: kadowaki@kuhp.kyoto-u.ac.jp

The online version of this article contains supplemental material.

Abbreviations used in this article: ALDH, aldehyde dehydrogenase; ALDH1A2, aldehyde dehydrogenase 1 family, member A2; cDC, conventional dendritic cell; CLA, cutaneous lymphocyte Ag; DC, dendritic cell; DEAB, diethylaminobenzaldehyde; GUSB, β-glucuronidase; mDC, myeloid DC; MFI, mean fluorescence intensity; MLN, mesenteric lymph node; MoDC, monocyte-derived DC; pDC, plasmacytoid DC; PE-Cy5, PE-Cyanin 5; RA, all-*trans*-retinoic acid; RALDH, retinal dehydrogenase; RAR, pan-RA receptor; rh, recombinant human; Treg, regulatory T; VD_3, 1α,25-dihydroxyvitamin D_3; VDR, vitamin D receptor.

www.jimmunol.org/cgi/doi/10.4049/jimmunol.1203517

In the current study, we used human DCs from blood and MLNs, as well as DCs induced from monocytes or $CD34^+$ progenitors in vitro, and explored 1) DC subsets that express a high level of RALDH2, 2) factors that induce human DCs to express a high level of RALDH2, 3) differences between humans and mice in RA-producing DC subsets and RA-inducing factors, 4) intracellular mechanisms by which RALDH2 is induced in DCs, and 5) T cell responses induced by RA-producing DCs in an RA-dependent manner. To quantify the activity of RALDH in mouse (2, 4, 5, 7, 8, 12, 19) and human (5, 19) DCs, recent studies used the Aldefluor reagent that freely diffuses into cells and is converted to a fluorescent product by aldehyde dehydrogenase (ALDH) activity. Thus, we used this reagent in combination with quantitation of ALDH1A2 mRNA to quantify the RA-producing capacity of DCs. We found that only $CD1c^+$ mDCs are capable of expressing a high level of RALDH2 in response to 1α,25-dihydroxyvitamin D_3 (VD_3) together with GM-CSF and that the $RALDH2^{high}$ mDCs induce T cells to preferentially express gut-homing molecules and Th2 cytokines in an RA-dependent manner. This study thus reveals a previously unrecognized distinctive function of human $CD1c^+$ mDCs and an unexpected role of vitamin D, that is, induction of RA from human DCs.

Materials and Methods

Culture media

RPMI 1640 (Nacalai tesque) supplemented with 10% heat-inactivated FCS (ThermoTrace), 2 mM L-glutamine, penicillin G, streptomycin (Life Technologies), and 10 mM HEPES were used for cell culture.

Reagents

Reagents and sources were as follows: recombinant human (rh)TNF, rhIL-3, rh stem cell factor, rhFLT3 ligand (PeproTech); rhGM-CSF (sargramostim; Genzyme); R848 (InvivoGen); LPS (from *Escherichia coli* O111:B4; Sigma-Aldrich); PGE_2 (MP Biomedicals); rhIL-2 (teceleukin; Shionogi & Co.); recombinant mouse GM-CSF (Kirin Brewery); anti-human IL-4 (clone MP4-25D2; eBioscience); anti-human CD28 mAbs (BD Biosciences); LE540 (Wako); U0126 (Cayman Chemical); SB203580, SP600125 (InvivoGen); VX-745 (Tocris); JAK inhibitor I (pyridone 6; Calbiochem); and SB239063 (Enzo Life Sciences). The inhibitors were dissolved in DMSO. Immunomodulatory factors added to DCs are listed in Table I. The following reagents were used for ELISA: anti–human IFN-γ mAb (clone 2G1 as capture Ab), biotinylated anti–human IFN-γ mAb (as detection Ab) and HRP-conjugated streptavidin (Endogen), OptEIA human IL-4 and IL-10 ELISA set (BD Biosciences), human IL-5 ELISA MAX Standard set (BioLegend), and a human IL-13 CytoSets kit (BioSource International).

The following Abs were used to stain human cells and are denoted as "fluorochrome-Ag." FITC-CD45RO, CD14, CD16, CD20, β_7 integrin, and cutaneous lymphocyte Ag (CLA), Alexa Fluor 488-CD1c, PE-CD103, α_4 integrin, and CD203c, PE-Cyanin 5 (PE-Cy5)-CD4, PE-Cyanin 7-CD4, and Brilliant Violet 421-CD11c were from BioLegend; FITC-CD3 and HLA-DR, PE-CD11c and CD25, and PE-Cy5-CD11c from BD Biosciences; allophycocyanin-CD141 from Miltenyi Biotec; allophycocyanin-CCR9 (clone 248621) were from R&D Systems.

The following Abs were used to stain mouse cells and are denoted as fluorochrome-Ag. FITC-B220, PE-CD11c, and allophycocyanin-CD8 were from BD Biosciences; allophycocyanin-CD103 were from BioLegend.

Cell preparations

This study was approved by the Institutional Review Board at Graduate School of Medicine, Kyoto University, and abides by the tenets of the Declaration of Helsinki. All specimens from humans were obtained from healthy donors and patients with written informed consent. To isolate human blood DCs, total PBMCs were depleted of $CD3^+$, $CD14^+$, and $CD16^+$ cells using Dynabeads goat anti-mouse IgG (Invitrogen Dynal). Then, $CD4^+CD11c^+CD141^{-/low}lin^-$ cells ($CD1c^+$ mDCs), $CD4^+CD141^{high}lin^-$ cells ($CD141^{high}$ mDCs), and $CD4^+CD11c^-CD141^{-/low}lin^-$ cells (pDCs) were purified using FACSAria cell sorter (BD Biosciences) (Supplemental Fig. 1A). The expression of CD1c on sorted blood $CD1c^+$ mDCs, $CD141^{high}$ mDCs, and pDCs is shown in Supplemental Fig. 1B. More than 98% of sorted cells were HLA-DR positive (Supplemental Fig. 1C). $CD203c^+$ basophils were isolated by sorting. Naive $CD4^+$ T cells and resting Treg cells (20) were $CD4^{high}CD25^-CD45RO^-$ cells and $CD4^{high}CD25^+CD45RO^-$ cells, respectively. Reanalysis of the sorted cells confirmed a purity of >98%. $CD8^+$ T cells were isolated from PBMCs using CD8 MicroBeads (Miltenyi Biotec).

Human MLNs from patients with colon cancer or Crohn's disease were obtained at Kyoto University Hospital or Hyogo College of Medicine Hospital, respectively. Single-cell suspension of MLNs was obtained by digestion with 500 μg/ml collagenase IV (Wako) and DNase I (Sigma-Aldrich) for 30 min, followed by sorting $CD4^+CD11c^+CD103^+lin^-CD141^{low/int}$ ($CD103^+$ mDCs), $CD4^+CD11c^+CD103^-lin^-CD141^{low/int}$ ($CD103^-$ mDCs), and $CD4^+CD11c^-CD103^-lin^-CD141^{low/int}$ (pDCs) as sorting strategy for blood DCs (Supplemental Fig. 1D). More than 99% of sorted cells were HLA-DR positive (Supplemental Fig. 1E).

Mouse $CD8^+$ and $CD8^-$ splenic DCs were prepared from BALB/c mice as described previously (Supplemental Fig. 1F) (21).

Single-cell suspensions from BALB/c mouse MLNs were prepared by collagenase (Boehringer-Ingerheim) digestion. Low-density cells were separated with BSA gradient centrifugation (Sigma-Aldrich), stained with PE-conjugated anti-CD11c, FITC-conjugated anti-B220, and allophycocyanin-conjugated anti-CD103 mAbs. DCs were first positively enriched using anti-PE microbeads (Mitenyi Biotec), and then, $CD103^+CD11c^+B220^-$ cells and $CD103^-CD11c^+B220^-$ cells were isolated as $CD103^+$ cDCs and $CD103^-$ cDCs, respectively (Supplemental Fig. 1G).

Cell culture

Human blood $CD1c^+$ mDCs, $CD141^{high}$ mDCs, and monocytes were cultured with 800 U/ml GM-CSF for 2 d. Blood pDCs were cultured with 10 ng/ml IL-3 for 2 d. Human mDCs and mouse cDCs from MLNs were cultured with 800 U/ml GM-CSF for 24 h. Human MLN pDCs were cultured with 10 ng/ml IL-3 for 24 h. Mouse splenic cDCs were cultured with 800 U/ml GM-CSF for 24 h. During these cultures, soluble factors (reagents in Table I, TLR ligands, TNF, PGE_2, LE540, or pharmacological inhibitors) were added as indicated. Concentrations of the reagents other than those listed on Table I were 10 μg/ml R848, 1 μg/ml LPS, 100 ng/ml Pam_3CSK_4, 10 ng/ml TNF, 1 μg/ml PGE_2, 1 μM LE540, 20 μM SB203580, 10 μM SP600125, and 20 μM U0126. LE540 and the pharmacological inhibitors were added to the cultures 30 min before adding other reagents. To quantify cell viability, the percentages of propidium iodide–negative cells were measured by flow cytometry after cell debris was excluded by appropriate forward scatter thresholds.

Generation of DCs from monocytes and $CD34^+$ progenitor cells

Monocytes were purified from PBMCs using CD14 MicroBeads (Miltenyi Biotec) and cultured with 800 U/ml GM-CSF and 500 U/ml IL-4 for 7 d to induce immature monocyte-derived DCs (MoDCs). LPS (100 ng/ml) was added during the last 2 d to induce maturation. Immunomodulatory factors (Table I) were added during the whole culture periods. To generate umbilical cord blood $CD34^+$ progenitor cell–derived DCs, $CD34^+$ cells were isolated using CD34 MicroBeads (Miltenyi Biotec) from cord blood and were cultured with 20 ng/ml stem cell factor, 50 ng/ml FLT3 ligand, 800 U/ml GM-CSF, and 2.5 ng/ml TNF for 7 d. Then, the cells were cultured in the absence or presence of RA, VD_3, or LPS (1 μg/ml) for 2 d.

Aldefluor assays and analysis of surface molecules

ALDH activity was determined using the Aldefluor staining kit (StemCell Technology) according to the manufacturer's protocol. Diethylaminobenzaldehyde (DEAB) (Wako) was used as an ALDH inhibitor. T cells cocultured with DCs were stained with mAbs for α_4 integrin, β_7 integrin, CLA, or CCR9. Live cells gated as propidium iodide–negative cells were acquired by FACSCalibur (BD Biosciences). Data were analyzed with FlowJo (Tree Star).

Reverse transcription and real-time PCR

$CD1c^+$ mDCs, $CD141^{high}$ mDCs, and pDCs were cultured with indicated stimuli for 24 h. Total RNA was isolated using Homogenizer and the PureLink RNA Micro Kit (Invitrogen). First-strand cDNA synthesis was performed with the ReverTra Ace qPCR RT Kit (Toyobo). Real-time PCR was performed on the Thermal Cycler Dice Real-Time System (TaKaRa). ALDH1A1, ALDH1A2, ALDH1A3, CYP27B1, vitamin D receptor (VDR), and β-glucronidase (GUSB) were detected using TaqMan Gene Expression Assays (Applied Biosystems) and THUNDERBIRD Probe qPCR Mix (Toyobo). Primer and probe sets were as follows: *ALDH1A1*, Hs00946916_m1; *ALDH1A2*, Hs00180254_m1; *ALDH1A3*, Hs00167476_m1; *CYP27B1*, Hs00168017_m1; *VDR*, Hs01045840_m1; and *GUSB*, Hs00930627_m1.

The mRNA expression levels of each gene were normalized to those of *GUSB*.

T cell cultures with DCs

After extensive wash, CD1c$^+$ mDCs (1×10^4 cells) cultured with GM-CSF, RA, or VD_3 for 2 d were cocultured with allogeneic naive CD4$^+$ T cells or total CD8$^+$ T cells (1×10^5 cells) in the absence or presence of 1 μM LE540, 10 μg/ml rat IgG1, or 10 μg/ml anti–IL-4 mAb in 96-well U-bottom plates for 6 d. IL-2 (10 U/ml) was added to CD8$^+$ T cell culture. The CD4$^+$ T cells were restimulated at 1×10^6 cells/ml with plate-bound anti-CD3 (OKT3) and 1 μg/ml soluble anti-CD28 mAbs in 96-well flat-bottom plates for 24 h. The supernatants were analyzed for cytokines by ELISA.

Statistical analysis

Data are presented as the mean ± SE. Statistical comparisons were performed using paired two-tailed *t* test. Difference with $p < 0.05$ was considered significant.

Results

Human blood CD1c$^+$ mDCs, but not CD141^{high} mDCs, express a high level of RALDH2 in response to GM-CSF and VD_3

In search of human DCs that express a high level of RALDH enzymes, different subsets of blood DCs were treated with various factors that have been reported to modulate immunostimulatory activity of DCs (Table I), and ALDH activity was measured with Aldefluor (2, 4, 5, 7, 8, 12, 19). To keep mDCs alive, we added GM-CSF (22) to CD1c$^+$ mDCs. GM-CSF by itself induced little ALDH activity (Fig. 1A, 1B). Adding RA with GM-CSF only slightly induced the activity, whereas VD_3, which modulates immunostimulatory properties of human mDCs and MoDCs (23–25), together with GM-CSF strongly upregulated the ALDH activity in CD1c$^+$ mDCs. RA plus VD_3 further augmented it (Fig. 1A, 1B). RA and VD_3 without GM-CSF induced little ALDH activity (Fig. 1A), indicating that GM-CSF is necessary for the induction. Ligands for TLRs (R848, LPS, and Pam_3CSK_4) and TNF strongly suppressed the ALDH activity, but PGE_2, which has been reported to suppress the ALDH activity in mouse bone marrow DCs (19), did not (Fig. 1C). There were no substantial differences in cell viability between different culture conditions at the time of harvest (data not shown). None of the other immunomodulatory factors (Table I) upregulated the ALDH activity in combination with GM-CSF (Supplemental Fig. 2).

In contrast to CD1c$^+$ mDCs, CD141^{high} mDCs (Fig. 1D), pDCs (Fig. 1E), and CD34-derived DCs (Fig. 1F) cultured with RA and VD_3 exhibited little ALDH activity. RA and VD_3 without or with LPS slightly induced ALDH activity in MoDCs but at far lower levels than that in CD1c$^+$ mDCs (Fig. 1G). Consistent with a previous observation that human basophils express RALDH2 in response to IL-3 (26), IL-3 alone induced ALDH activity in basophils, but there was no augmentation with RA and VD_3 (Fig. 1H). There were no substantial differences in cell viability between different culture conditions (data not shown). Again, none of the other factors (Table I) upregulated the ALDH activity in combination with GM-CSF (CD141^{high} mDCs, MoDCs) or IL-3 (pDCs) (Supplemental Fig. 2).

We also cultured monocytes with GM-CSF in the absence or presence of the immunomodulatory factors (Table I). RA plus VD_3 substantially induced ALDH activity, albeit to a lesser extent than that in CD1c$^+$ mDCs. None of the other factors substantially induced the activity (Supplemental Fig. 2).

We next examined whether the ALDH activity detected by Aldefluor correlates with the expression levels of mRNA for *ALDH1A2* (encoding RALDH2) in CD1c$^+$ mDCs, CD141^{high} mDCs, and pDCs. Consistent with the results by Aldefluor analyses, GM-CSF alone induced little expression of ALDH1A2 mRNA in CD1c$^+$ mDCs, and the addition of VD_3 markedly upregulated it (Fig. 1I). The addition of RA to GM-CSF and to GM-CSF plus VD_3 slightly increased the expression of ALDH1A2 mRNA, but R848 completely suppressed it. There was almost no expression of ALDH1A2 mRNA in CD141^{high} mDCs or pDCs. mRNAs for *ALDH1A1* and *ALDH1A3* (encoding RALDH1 and RALDH3) were hardly expressed in CD1c$^+$ mDCs even in the presence of the indicated stimulation (Fig. 1J, 1K).

Collectively, 1) CD1c$^+$ mDCs, but not the other human blood DC subsets, express a high level of RALDH2 in response to GM-CSF plus VD_3, and exogenous RA augments the expression, and 2) proinflammatory factors (TLR ligands and TNF) suppress the expression of RALDH2.

Human CD103$^-$ mDCs in MLNs gain ALDH activity in response to the VD_3-containing stimulus

To examine whether human MLN DCs exhibit ALDH activity as mouse MLN CD103$^+$ DCs do (3, 4), DC subsets were isolated from MLNs of patients with colon cancer or Crohn's disease in the same way as done for blood DCs (Supplemental Fig. 1D). Unlike in blood, CD141^{high} mDCs were not identified as a discrete population in MLNs. CD11c^{high} mDCs were subdivided into CD103$^+$ and CD103$^-$ mDCs. pDCs did not express CD103.

Unlike mouse MLN DCs, freshly isolated human CD103$^+$ MLN mDCs did not have ALDH activity (Fig. 2). Unexpectedly, CD103$^-$ but not CD103$^+$ MLN mDCs gained a high level of ALDH activity in response to GM-CSF, RA, and VD_3. pDCs did not exhibit ALDH activity. All the above results were the same in DCs from both colon cancer and Crohn's disease. Thus, in humans, CD103$^-$ but not CD103$^+$ MLN mDCs may be RA-producing DCs in situ in the intestine.

Mouse splenic and MLN cDCs gain ALDH activity in response to GM-CSF alone

Genome-wide expression profiling clustered human CD141^{high} mDCs and CD1c$^+$ mDCs with mouse CD8$^+$ cDCs and CD8$^-$ cDCs, respectively (18). Thus, we examined whether VD_3 differentially induces mouse splenic cDC subsets to gain ALDH activity. As we reported (4), GM-CSF alone was sufficient to induce high levels of ALDH activity in both CD8$^+$ DCs and CD8$^-$ DCs in the spleen (Fig. 3A). Neither RA nor VD_3 augmented the activity. Unlike in human CD1c$^+$ mDCs, LPS did not suppress it. There were no substantial differences in cell viability between different culture conditions (data not shown). We also examined ALDH activity in mouse MLN cDCs in the absence or presence of the VD_3-containing stimulus. As reported (3), fresh CD103$^+$ but not CD103$^-$ cDCs in MLNs exhibited ALDH activity (Fig. 3B). Again, GM-CSF alone was sufficient to induce high levels of ALDH activity in both CD103$^+$ and CD103$^-$ cDCs, and the addition of RA and VD_3 did not augment it.

Table I. Immunomodulatory factors added to DCs

Name	Concentrations	Sources
RA	10 nM	Wako
VD_3	10 nM	Wako
IFN-α	1000 U/ml	Intron A, Schering-Plough
IL-4	500 U/ml	PeproTech
TGF-β	10 ng/ml	PeproTech
Vasoactive intestinal peptide	100 nM	LKT Laboratories
Rosiglitazone	10 μM	Alexis Biochemicals
T0901317	1 μM	Cayman Chemicals
Rapamycin	100 ng/ml	PeproTech
Tacrolimus	100 ng/ml	Enzo Life Sciences
Cyclosporin A	1000 ng/ml	Sigma-Aldrich
Dexamethasone	1 μM	Sigma-Aldrich

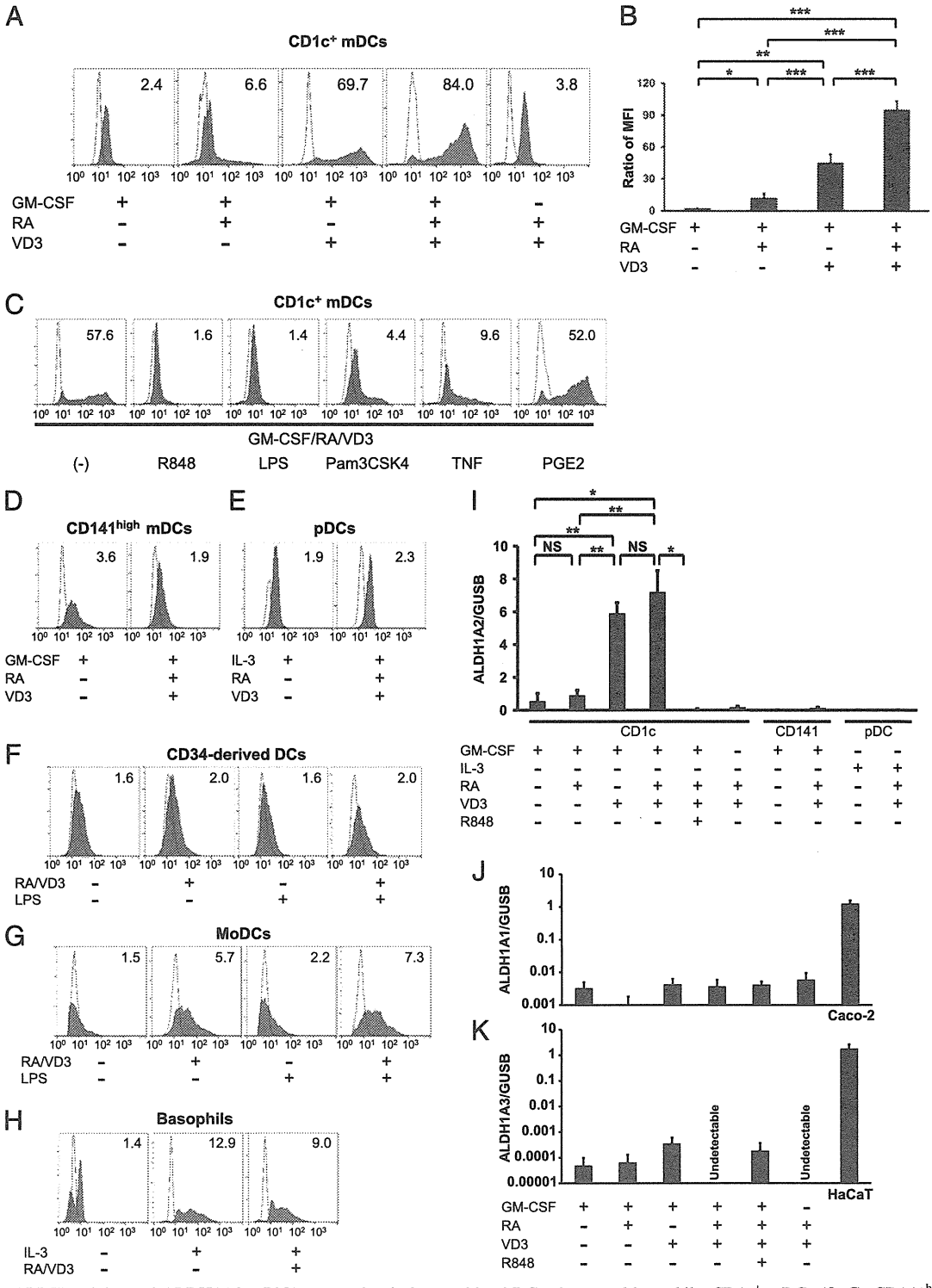

FIGURE 1. ALDH activity and ALDH1A2 mRNA expression in human blood DC subsets and basophils. CD1c$^+$ mDCs (**A**–**C**), CD141^{high} mDCs (**D**), pDCs (**E**), and basophils (**H**) were cultured in the absence or presence of the indicated reagents for 2 d. CD34$^+$ progenitor cell–derived dendritic cells (CD34-derived DCs) (**F**) and MoDCs (**G**) were cultured as indicated in *Materials and Methods*. The cells were incubated with Aldefluor in the absence (solid histograms) or presence (open histograms) of an ALDH inhibitor DEAB and were analyzed by flow cytometry. The numbers shown with each histogram represent ratios of mean fluorescence intensity of Aldefluor in the absence of DEAB to that in the presence of DEAB. (**I**) ALDH1A2 mRNA expression was measured by real-time RT-PCR. CD1c$^+$ mDCs, CD141^{high} mDCs, and pDCs were cultured with the indicated stimuli for 24 h. The expression levels were normalized to those of GUSB. $*p < 0.05$, $**p < 0.01$, $***p < 0.001$. ALDH1A1 (**J**) and ALDH1A3 (**K**) mRNA expressions were measured by real-time RT-PCR. CD1c$^+$ mDCs were cultured with the indicated stimuli for 24 h. Human colon cancer cell line Caco-2 and human keratinocyte cell line HaCaT were used as positive controls for ALDH1A1 and ALDH1A3, respectively. The expression levels were normalized to those of GUSB. Note the low levels of the scales. The data are representative of three (A, D–G) or two (H) independent experiments and are shown as the mean ± SE of 8 (B), 4 (I), or 3 (J, K) independent experiments.

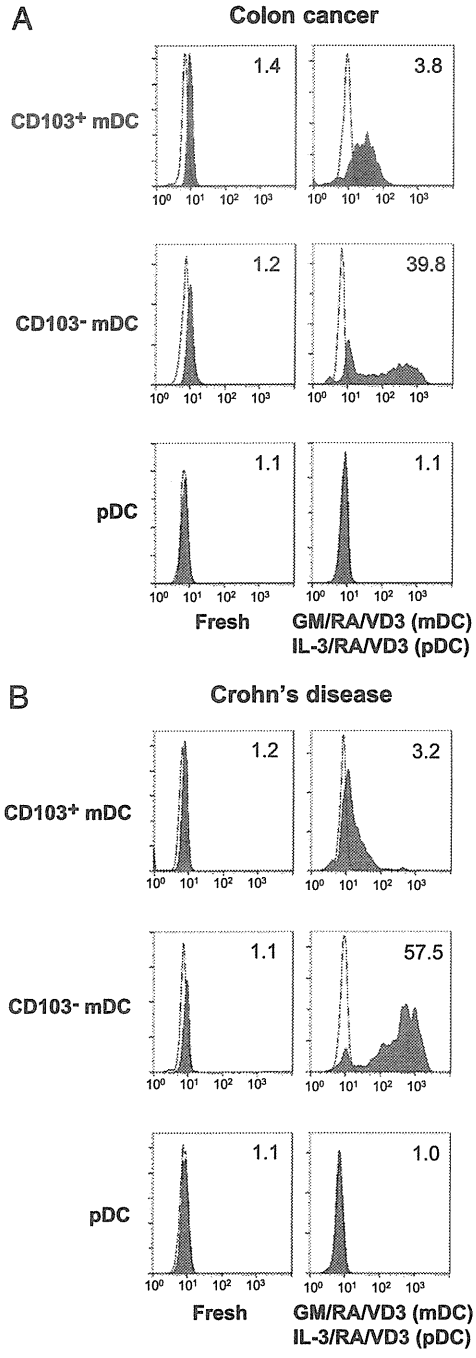

FIGURE 2. ALDH activity in human MLN DC subsets. $CD103^+$ mDCs, $CD103^-$ mDCs, or pDCs were purified from MLNs of patients with colon cancer (**A**) or Crohn's disease (**B**) and were analyzed without culture or after culture with the indicated stimuli for 24 h. Histograms and the numbers shown with them are presented as in Fig. 1. The data are representative of three (A) or two (B) independent experiments.

Collectively, the RA-producing DC subsets and the stimulation to induce RA production are different between human and mouse DCs, in that 1) both of the cDC subsets in mouse spleen ($CD8^+$ and $CD8^-$) and MLNs ($CD103^+$ and $CD103^-$) exhibit ALDH activity in response to GM-CSF alone, 2) VD_3 does not induce or increase the activity, and 3) TLR signaling does not suppress the activity in mice.

Engagement of RA receptor is necessary for the high level of RALDH2 expression induced by VD_3

We investigated the mechanisms by which GM-CSF, RA, and VD_3 induce a high level of RALDH2 in human $CD1c^+$ mDCs. Exogenous RA augmented the expression of RALDH2 induced by VD_3 (Fig. 1A, 1B). Thus, we examined whether endogenous RA is responsible for the induction of RALDH2 by VD_3. A pan-RA receptor (RAR) antagonist LE540 diminished the induction of ALDH activity by VD_3 (Fig. 4A), indicating that endogenous RA or possibly RAR agonists contained in the serum are necessary for the induction of a high level of RALDH2 by VD_3. However, the induction of RALDH2 by RA alone was much weaker than the induction by VD_3 (Fig. 1A, 1B), indicating that combined signals by RA and VD_3 are necessary for the full expression of RALDH2.

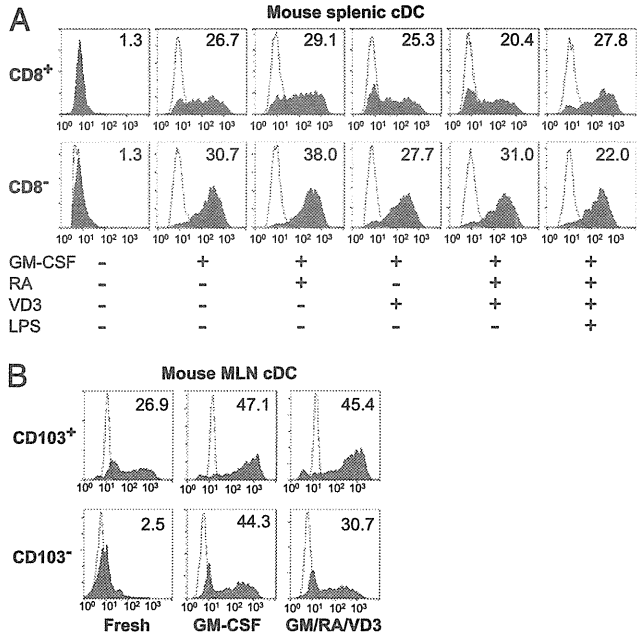

FIGURE 3. ALDH activity in mouse splenic and MLN cDC subsets. (**A**) $CD8^+$ and $CD8^-$ mouse splenic cDCs were cultured without or with the indicated stimuli for 24 h. (**B**) $CD103^+$ and $CD103^-$ mouse MLN cDCs were analyzed without culture or were cultured with the indicated stimuli for 24 h. Histograms and the numbers shown with them are presented as in Fig. 1. The data are representative of three independent experiments.

When cultured with GM-CSF, RA, and VD_3, $CD1c^+$ mDCs expressed only a low level of mRNA for CYP27B1, the enzyme that converts 25-hydroxyvitamin D_3 into its bioactive form VD_3 (27), although $CD1c^+$ mDCs expressed a high level of CYP27B1 mRNA in the presence of R848 (Supplemental Fig. 3A). Thus, endogenous VD_3 does not appear to participate in the induction of RALDH2.

$CD1c^+$ mDCs, $CD141^{high}$ mDCs, and pDCs expressed similar levels of mRNA for the nuclear VDR, consistent with a previous report (Supplemental Fig. 3B) (25). Thus, the marked effect of VD_3 on the induction of RALDH2 in $CD1c^+$ mDCs is not likely to be determined by differential expression of VDR among the DC subsets, but $CD1c^+$ mDCs may have distinctive molecular machineries to express RALDH2 in response to VD_3.

Activation of p38 is necessary for the induction of RALDH2

We investigated signaling pathways involved in the induction of RALDH2 in $CD1c^+$ mDCs. After stimulation with GM-CSF, RA, and VD_3, the DCs started to express ALDH1A2 mRNA at 6 h, and the expression reached its peak at 24 h (Fig. 4B). This slow kinetics indicates that the induction of ALDH1A2 mRNA is not due to direct transcriptional activity of VDR. Instead, secondary signals downstream of VDR and RAR are likely to mediate the induction of ALDH1A2 mRNA.

A pan-JAK inhibitor strongly blocked the induction of ALDH activity (Fig. 4C) in accord with the dependence of the induction

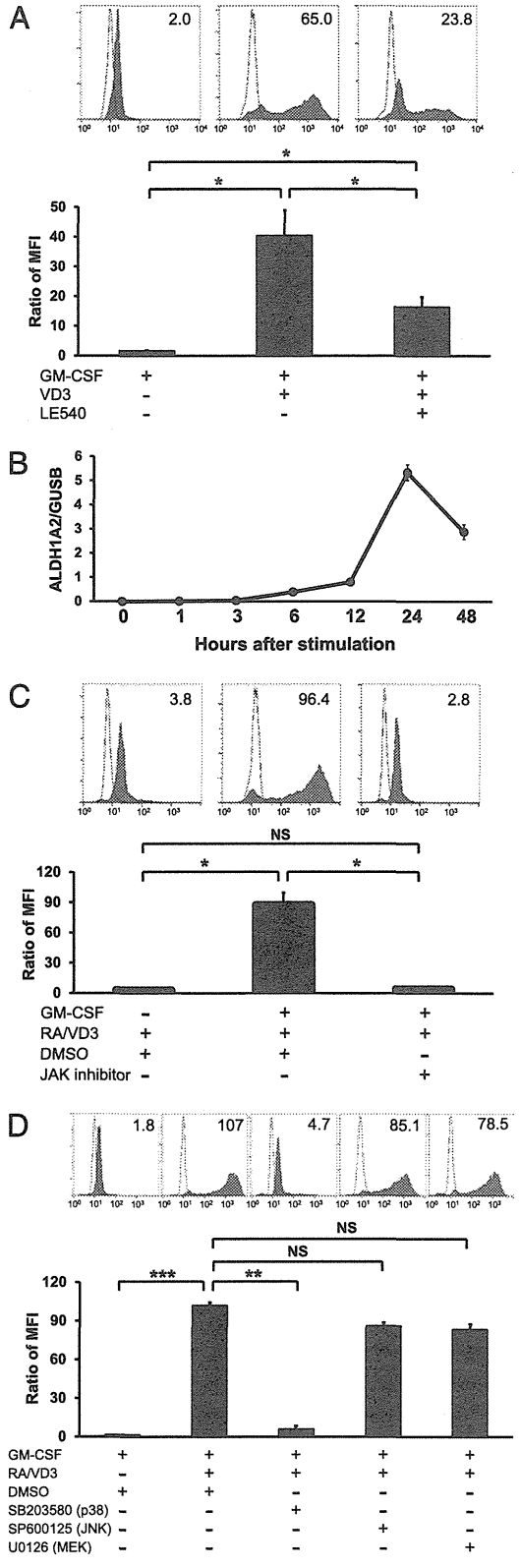

FIGURE 4. The induction of ALDH activity in CD1c$^+$ mDCs is dependent on RAR, JAK, and p38 signaling. (**A**, **C**, and **D**) CD1c$^+$ mDCs were cultured with the indicated reagents for 2 d. Histograms and the numbers shown with them are presented as in Fig. 1. The histograms are representative data, and the graphs show the mean ± SE of four (A) or three (C, D) independent experiments. (**B**) CD1c$^+$ mDCs were cultured with GM-CSF, RA, and VD_3 for the indicated time periods. ALDH1A2 mRNA expressions were measured by real-time RT-PCR. The expression levels were normalized to those of GUSB. The data are presented as the mean ± SD of duplicate samples in one of two independent experiments.

on GM-CSF. Three p38 MAPK inhibitors, SB203580 (Fig. 4D), SB239063 (28), and VX-745 (29) (data not shown), also blocked the induction. In contrast, inhibitors against JNK (SP600125) or MEK 1/2 (U0126) did not do so (Fig. 4D). There were no substantial differences in cell viability between different culture conditions (data not shown). Thus, RALDH2 in CD1c$^+$ mDCs is induced in a p38-dependent manner.

RALDH2^{high} mDCs induce T cells to acquire gut-homing capacities in an RA-dependent manner

RA derived from mouse intestinal DCs endows T cells with the expression of gut-homing molecules, $\alpha_4\beta_7$ integrin and CCR9 (1). Furthermore, intestinal DCs reciprocally suppress the expression of skin-homing molecules, P- and L-selectin ligands, on T cells (30). Thus, we examined homing properties of T cells stimulated with GM-CSF/RA/VD_3–treated RALDH2^{high}CD1c$^+$ mDCs (hereafter referred to as RALDH2^{high} mDCs). Naive CD4$^+$ T cells stimulated with allogeneic RALDH2^{high} mDCs expressed a higher level of $\alpha_4\beta_7$ integrin (Fig. 5A, 5B) and reciprocally a lower level of a P- and L-selectin ligand CLA (Fig. 5C) than T cells stimulated with GM-CSF–treated RALDH2^{low}CD1c$^+$ mDCs (hereafter referred to as RALDH2^{low} mDCs). The upregulation of $\alpha_4\beta_7$ integrin and downregulation of CLA by RALDH2^{high} mDCs were abrogated by LE540. These data indicate that RALDH2^{high} mDCs induce gut-homing and reduce skin-homing properties of T cells in an RA-dependent manner. RALDH2^{high} mDCs did not induce allogeneic naive CD4$^+$ T cells or total CD8$^+$ T cells to express a detectable level of CCR9 (data not shown).

RALDH2^{high} mDCs induce naive CD4$^+$ T cells to acquire Th2 cytokine–producing capacities in an RA-dependent manner

We examined cytokine-producing properties of naive CD4$^+$ T cells stimulated with allogeneic mDCs. CD4$^+$ T cells stimulated with RALDH2^{high} mDCs secreted significantly higher levels of Th2 cytokines IL-4, IL-5, and IL-13 than those stimulated with RALDH2^{low} mDCs (Fig. 6A). This effect was abrogated by LE540 (Fig. 6A), but not by anti–IL-4 neutralizing mAb (Fig. 6B). CD4$^+$ T cells stimulated with RALDH2^{high} mDCs secreted a similar level of IFN-γ, compared with those stimulated with RALDH2^{low} mDCs (Fig. 6C). CD4$^+$ T cells stimulated with RALDH2^{high} mDCs secreted a significantly higher level of IL-10 than those stimulated with RALDH2^{low} mDCs, but the induction of IL-10 was not abrogated by LE540 (Fig. 6C). These data indicate that RALDH2^{high} mDCs induce naive CD4$^+$ T cells to acquire the ability to produce high levels of Th2 cytokines in an RA-dependent and IL-4–independent manner.

We also examined whether naive CD4$^+$ T cells stimulated with RALDH2^{high} mDCs acquire regulatory activity. Although CD4$^+$ T cells stimulated with RALDH2^{high} mDCs slightly suppressed proliferation of concomitant T cells, the effect was much weaker than that exhibited by resting Treg cells directly purified from blood (20) (data not shown). Thus, RALDH2^{high} mDCs do not have an unambiguous regulatory T cell–inducing ability detectable by our assay.

Discussion

RA plays a critical role in maintaining immune homeostasis in the intestine (27). Human DCs that produce a high level of RA remained unknown. The present study identifies blood CD1c$^+$ mDCs as a DC subset that potently produces RA in response to VD_3 in humans. RALDH2^{high} CD1c$^+$ mDCs induced T cells to preferentially express gut-homing molecules and Th2 cytokines in an RA-dependent manner. This study reveals a novel component in

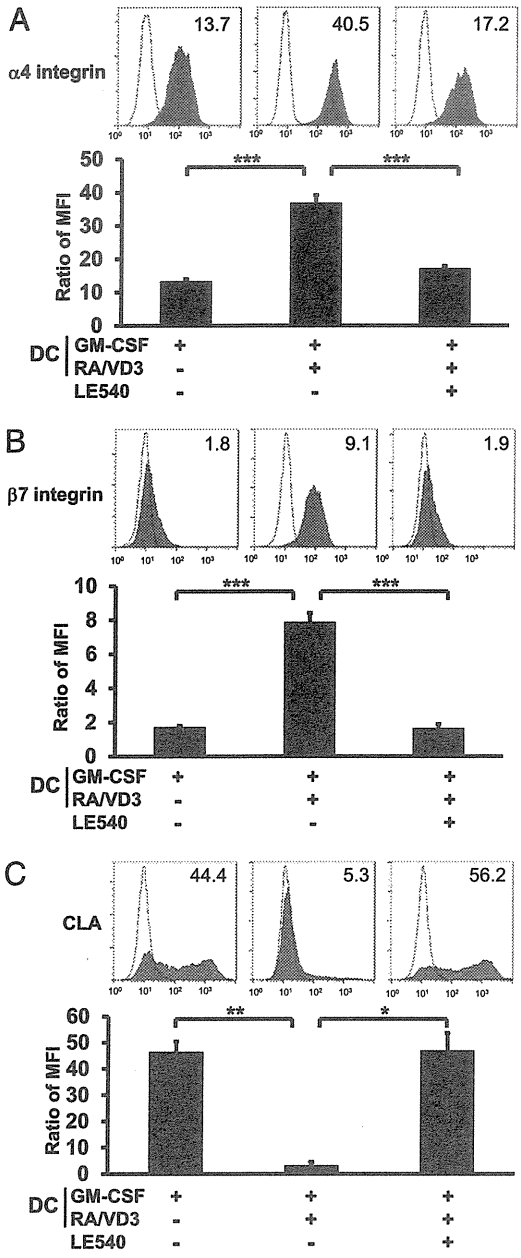

FIGURE 5. RALDH2^{high} mDCs induce gut-homing and suppress skin-homing molecules on CD4$^+$ T cells in an RA-dependent manner. CD1c$^+$ mDCs were cultured with GM-CSF alone (RALDH2^{low} mDCs) or GM-CSF, RA, and VD_3 (RALDH2^{high} mDCs) for 2 d. The DCs were collected and extensively washed. Then allogeneic naive CD4$^+$ T cells were stimulated with RALDH2^{low} mDCs or RALDH2^{high} mDCs in the absence or presence of LE540 for 6 d. The T cells were stained for α_4 integrin (**A**), β_7 integrin (**B**), or CLA (**C**). Open histograms represent cells stained with isotype-matched control mAbs. The numbers shown with each histogram represent ratios of mean fluorescence intensity (MFI) of each surface molecule to that of isotype-matched control. The histograms are representative data, and the graphs show the mean ± SE from six (A, B) or three (C) independent experiments. $*p < 0.05$, $**p < 0.01$, $***p < 0.001$.

the immune system in humans, that is, a "vitamin D – CD1c$^+$ mDC – RA" axis for immune regulation.

Which DCs produce RA will be determined by two factors: 1) environmental signals DCs receive, and 2) intrinsic nature of each DC subset. In mice, RA (4–8), GM-CSF (4), IL-4 (4, 9), and TLR ligands (2, 4, 5, 10–12) induce DCs to express RALDH2. In humans, RA (5), Pam_3CSK_4 (5, 12), and a peroxisome proliferator–activated receptor γ ligand (rosiglitazone) (31) augment the expression of RALDH2 in MoDCs. In this study, to our knowledge, we demonstrated for the first time that VD_3 induces CD1c$^+$ mDCs to express a high level of RALDH2 in the presence of GM-CSF. Whereas exogenous RA moderately augmented the induction, neither IL-4 nor various immunomodulatory reagents including rosiglitazone augmented it. Notably, proinflammatory factors, TLR ligands and TNF, strongly suppressed ALDH activity. These data suggest that VD_3 is a key factor to induce human CD1c$^+$ mDCs to express RALDH2 in the steady state.

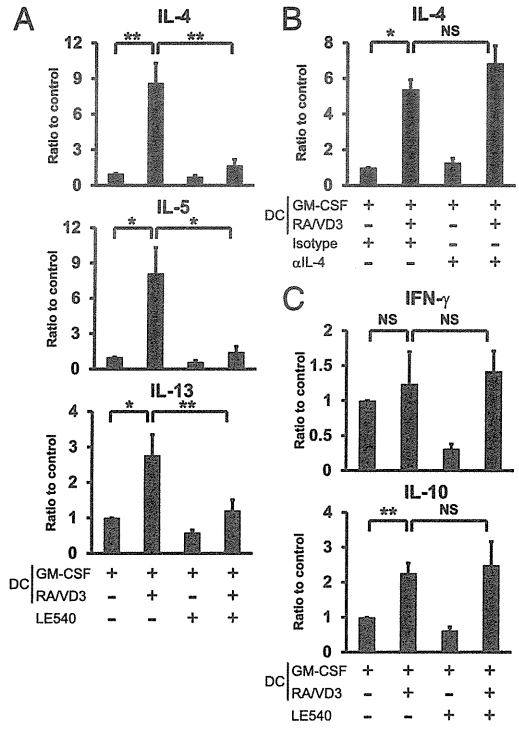

FIGURE 6. RALDH2^{high} mDCs induce CD4$^+$ T cells to produce Th2 cytokines in an RA-dependent manner. CD1c$^+$ mDCs were cultured as in Fig. 5 and were collected and extensively washed. Then allogeneic naive CD4$^+$ T cells were cocultured with RALDH2^{low} mDCs or RALDH2^{high} mDCs in the absence or presence of LE540 for 6 d (**A**, **C**) or in the presence of rat IgG1 (isotype) or anti–IL-4 mAb (**B**). The stimulated T cells were restimulated for 24 h, and the supernatants were analyzed for cytokines by ELISA. The data are normalized to the value obtained from CD4$^+$ T cells cocultured with RALDH2^{low} mDCs in the absence of LE540 or anti–IL-4 mAb. The data are shown as the mean ± SE of eight (A, C) or three (B) independent experiments. $*p < 0.05$, $**p < 0.01$. The mean and ranges of absolute cytokine concentrations from T cells cocultured with RALDH2^{low} mDCs in the absence of LE540 or anti–IL-4 mAb were as follows: (A) IL-4, 79.5 pg/ml (46.8–145 pg/ml); IL-5, 57.9 pg/ml (15.6–122 pg/ml); IL-13, 1720 pg/ml (321–4547 pg/ml); (B) IL-4, 63.9 pg/ml (42.9–104 pg/ml); and (C) IFN-γ, 28.5 ng/ml (9.48–80.6 ng/ml), and IL-10, 219 pg/ml (93.6–416 pg/ml).

It has been shown that VD_3 inhibits the expression of RALDH2 in mouse DCs (32). In addition, VD_3 represses RA-transcriptional activity via VDR in human myeloid cells (33). These findings indicate that VD_3 antagonizes the activity of RA. Thus, the cooperation between exogenous VD_3 and endogenously induced RA for the induction of RALDH2 in human CD1c$^+$ mDCs was unexpected. These results indicate that signaling pathways triggered by RA and VD_3 may antagonize or synergize, depending on cell types, coexisting factors, and/or species.

Among the human DC subsets we examined, CD1c$^+$ mDCs was the only subset that expresses a high level of RALDH2 in response to VD_3. Human CD141^{high} mDCs and their equivalent, mouse CD8$^+$CD11b$^-$ cDCs in lymphoid tissues (18) and CD103$^+$ cDC in

nonlymphoid tissues (17), share capacities to efficiently cross-present Ags to $CD8^+$ T cells (14–17). In contrast, distinctive functions of $CD1c^+$ mDCs, an equivalent of mouse $CD8^-CD11b^+$ cDCs (18), have been elusive. The present study suggests that, in contrast to $CD141^{high}$ mDCs, $CD1c^+$ mDCs may function as immunoregulatory DCs by preferentially producing RA upon exposure to VD_3.

Although several studies have shown that human MoDCs express RALDH2 (5, 12, 19, 31), gene expression profiling has shown that MoDCs markedly differ from the three subsets of human DCs in blood and lymphoid tissues and are more similar to macrophages (18). In addition, it remains to be determined to what extent monocytes differentiate into DCs in vivo in humans. Thus, the RALDH2 expression in $CD1c^+$ mDCs is likely to be more relevant to DC biology in vivo than that in MoDCs. Intriguingly, monocytes but not MoDCs exhibited a substantial level of ALDH activity in response to GM-CSF, RA, and VD_3, suggesting that $CD1c^+$ mDCs and monocytes may have similar machinery to express RALDH2.

Whereas freshly isolated mouse intestinal $CD103^+$ DCs but not $CD103^-$ DCs produce RA (3), we showed that 1) freshly isolated human MLN DCs do not have ALDH activity and that 2) $CD103^-$ mDCs but not $CD103^+$ mDCs in MLNs gain a high level of ALDH activity in response to the VD_3-containing stimulus. Although our data does not clarify the relationship between mouse and human DC subsets in MLNs, the data suggest that CD103 may not be a marker of DCs that preferentially produce RA in human MLNs. Jaesson et al. (34) reported that $CD103^+$ DCs from human MLNs induce T cells to express $\alpha_4\beta_7$ integrin and CCR9 in an RAR signaling–dependent manner. However, such DCs neither exhibited ALDH activity (Fig. 2A, 2B) nor induced T cells to express these gut-homing molecules (data not shown) in our experiments. Because Jaesson et al. (34) did not directly examine ALDH activity of MLN DCs, the reason for the discrepancy between the two studies is not clear.

Furthermore, GM-CSF alone was sufficient to induce high levels of ALDH activity in both of the cDC subsets in mouse spleen ($CD8^+$ and $CD8^-$) and MLNs ($CD103^+$ and $CD103^-$), and VD_3 did not augment the activity. Thus, DC subsets capable of acquiring ALDH activity and the stimulation to induce DCs to acquire the activity appear to be significantly different between humans and mice.

RA (5) or zymosan (11) induces mouse splenic DCs to express RALDH2 through RAR or TLR2, respectively, in an ERK-dependent manner. Pam_3CSK_4 induces mouse splenic DCs to express RALDH2 in a JNK-dependent manner (12). In contrast, we showed that p38 but not MEK or JNK is necessary to induce human $CD1c^+$ mDCs to express RALDH2 in response to VD_3. Thus, although MAPK is important for the induction of RALDH2 in DCs, it appears that which MAPK is involved depends on the type of stimuli and/or species.

Although $RALDH2^{high}$ $CD1c^+$ mDCs induced the expression of a higher level of $\alpha_4\beta_7$ integrin and reciprocally suppressed the expression of CLA on T cells in an RA-dependent manner, we could not observe the induction of CCR9 in the culture conditions we used. Spiegl et al. (26) also reported no CCR9 induction on human T cells by RA. Thus, the induction of CCR9 on human T cells may be more tightly regulated than that on mouse T cells.

VD_3 directly acts on T cells to induce skin-homing receptors (35). The present study showed that VD_3 induces T cells to express gut-homing receptors through inducing RA production by DCs. It appears to be difficult to reconcile these two phenomena. A possible scenario is that $CD1c^+$ mDCs are exposed to VD_3 in peripheral tissues, migrate into regional lymph nodes, and present RA to T cells. Indeed, tissue-resident cells such as epithelial cells and macrophages (36) express CYP27B1. As such, exposure of DCs to VD_3 may be spatially and chronologically separated from T cell stimulation by the DCs.

VD_3 and RA have been thought to reciprocally control immune responses in the skin and intestine (27). Thus, the induction of RALDH2 by VD_3 is counterintuitive. However, such dichotomy between VD_3 and RA are becoming blurred. On the one hand, VD_3 locally produced by epithelial cells and macrophages in various organs and lymphoid tissues (36) likely has an immunomodulatory effect in a paracrine manner (37). On the other hand, RA-producing DCs exist in extraintestinal as well as intestinal tissues and their corresponding draining lymph nodes (2). In addition, a wide variety of cells can produce GM-CSF. Thus, VD_3, RA, and GM-CSF are likely to have opportunities to collaborate and to stimulate $CD1c^+$ mDCs in various tissues, and such DCs may induce gut-homing T cells by producing RA in extraintestinal as well as intestinal compartments.

$RALDH2^{high}$ mDCs induced naive $CD4^+$ T cells to acquire the ability to produce Th2 cytokines in an RA-dependent and IL-4–independent manner. The apparently direct effect of RA on Th2 induction is consistent with our previous report with mice (38). It has been shown that RA derived from basophils also induces Th2 cells (26). Thus, RA derived from $CD1c^+$ mDCs as well as basophils may contribute to Th2 polarization.

It has been proposed that Th2-type allergic responses may constitute an important asset of the immune system to maintain tissue homeostasis by ameliorating inflammation and promoting tissue repair (39, 40). The present study suggests that locally produced VD_3 may induce RA-producing $CD1c^+$ mDCs that promote a "type 2" environment, thus contributing to maintaining tissue homeostasis. Inflammation caused by infections, exemplified by the stimulation of $CD1c^+$ mDCs with TLR ligands and TNF, may extinguish the Th2-inducing RA production, and turn on type 1 inflammation. Taken together with a recent report that VD_3-stimulated $CD1c^+$ blood mDCs produce IL-10 and induce Treg cells (41), $CD1c^+$ mDCs may represent a DC subset that maintains immune homeostasis. Furthermore, epidemiological studies have shown that a poor vitamin D status is associated with an increased risk of autoimmune diseases (37). Thus, it is intriguing to speculate that RA production by $CD1c^+$ mDCs stimulated with VD_3 contributes to prevention of autoimmune diseases in the steady state.

In conclusion, this study reveals a novel link between two key immunomodulatory vitamins (vitamin A and D) via a distinctive human DC subset, that is, $CD1c^+$ mDCs. This may constitute a previously unrecognized immune component for maintaining tissue homeostasis. Exploiting immunomodulatory activity of this component may lead to novel therapies or prevention of various autoimmune or inflammatory disorders.

Acknowledgments

We thank Keiko Fukunaga for excellent technical assistance.

Disclosures

The authors have no financial conflicts of interest.

References

1. Iwata, M., A. Hirakiyama, Y. Eshima, H. Kagechika, C. Kato, and S.-Y. Song. 2004. Retinoic acid imprints gut-homing specificity on T cells. *Immunity* 21: 527–538.
2. Guilliams, M., K. Crozat, S. Henri, S. Tamoutounour, P. Grenot, E. Devilard, B. de Bovis, L. Alexopoulou, M. Dalod, and B. Malissen. 2010. Skin-draining lymph nodes contain dermis-derived $CD103^-$ dendritic cells that constitutively produce retinoic acid and induce $Foxp3^+$ regulatory T cells. *Blood* 115: 1958–1968.
3. Coombes, J. L., K. R. R. Siddiqui, C. V. Arancibia-Cárcamo, J. Hall, C.-M. Sun, Y. Belkaid, and F. Powrie. 2007. A functionally specialized population of mu-

cosal CD103$^+$ DCs induces Foxp3$^+$ regulatory T cells via a TGF-β and retinoic acid-dependent mechanism. *J. Exp. Med.* 204: 1757–1764.
4. Yokota, A., H. Takeuchi, N. Maeda, Y. Ohoka, C. Kato, S.-Y. Song, and M. Iwata. 2009. GM-CSF and IL-4 synergistically trigger dendritic cells to acquire retinoic acid-producing capacity. *Int. Immunol.* 21: 361–377.
5. Villablanca, E. J., S. Wang, J. de Calisto, D. C. O. Gomes, M. A. Kane, J. L. Napoli, W. S. Blaner, H. Kagechika, R. Blomhoff, M. Rosemblatt, et al. 2011. MyD88 and retinoic acid signaling pathways interact to modulate gastrointestinal activities of dendritic cells. *Gastroenterology* 141: 176–185.
6. Feng, T., Y. Cong, H. Qin, E. N. Benveniste, and C. O. Elson. 2010. Generation of mucosal dendritic cells from bone marrow reveals a critical role of retinoic acid. *J. Immunol.* 185: 5915–5925.
7. Molenaar, R., M. Knippenberg, G. Goverse, B. J. Olivier, A. F. de Vos, T. O'Toole, and R. E. Mebius. 2011. Expression of retinaldehyde dehydrogenase enzymes in mucosal dendritic cells and gut-draining lymph node stromal cells is controlled by dietary vitamin A. *J. Immunol.* 186: 1934–1942.
8. Jaensson-Gyllenbäck, E., K. Kotarsky, F. Zapata, E. K. Persson, T. E. Gundersen, R. Blomhoff, and W. W. Agace. 2011. Bile retinoids imprint intestinal CD103$^+$ dendritic cells with the ability to generate gut-tropic T cells. *Mucosal Immunol.* 4: 438–447.
9. Elgueta, R., F. E. Sepulveda, F. Vilches, L. Vargas, J. R. Mora, M. R. Bono, and M. Rosemblatt. 2008. Imprinting of CCR9 on CD4 T cells requires IL-4 signaling on mesenteric lymph node dendritic cells. *J. Immunol.* 180: 6501–6507.
10. Uematsu, S., K. Fujimoto, M. H. Jang, B.-G. Yang, Y.-J. Jung, M. Nishiyama, S. Sato, T. Tsujimura, M. Yamamoto, Y. Yokota, et al. 2008. Regulation of humoral and cellular gut immunity by lamina propria dendritic cells expressing Toll-like receptor 5. *Nat. Immunol.* 9: 769–776.
11. Manicassamy, S., R. Ravindran, J. Deng, H. Oluoch, T. L. Denning, S. P. Kasturi, K. M. Rosenthal, B. D. Evavold, and B. Pulendran. 2009. Toll-like receptor 2-dependent induction of vitamin A-metabolizing enzymes in dendritic cells promotes T regulatory responses and inhibits autoimmunity. *Nat. Med.* 15: 401–409.
12. Wang, S., E. J. Villablanca, J. De Calisto, D. C. O. Gomes, D. D. Nguyen, E. Mizoguchi, J. C. Kagan, H.-C. Reinecker, N. Hacohen, C. Nagler, et al. 2011. MyD88-dependent TLR1/2 signals educate dendritic cells with gut-specific imprinting properties. *J. Immunol.* 187: 141–150.
13. Ziegler-Heitbrock, L., P. Ancuta, S. Crowe, M. Dalod, V. Grau, D. N. Hart, P. J. M. Leenen, Y.-J. Liu, G. MacPherson, G. J. Randolph, et al. 2010. Nomenclature of monocytes and dendritic cells in blood. *Blood* 116: e74–e80.
14. Jongbloed, S. L., A. J. Kassianos, K. J. McDonald, G. J. Clark, X. Ju, C. E. Angel, C.-J. J. Chen, P. R. Dunbar, R. B. Wadley, V. Jeet, et al. 2010. Human CD141$^+$ (BDCA-3)$^+$ dendritic cells (DCs) represent a unique myeloid DC subset that cross-presents necrotic cell antigens. *J. Exp. Med.* 207: 1247–1260.
15. Poulin, L. F., M. Salio, E. Griessinger, F. Anjos-Afonso, L. Craciun, J.-L. Chen, A. M. Keller, O. Joffre, S. Zelenay, E. Nye, et al. 2010. Characterization of human DNGR-1$^+$BDCA3$^+$ leukocytes as putative equivalents of mouse CD8α+ dendritic cells. *J. Exp. Med.* 207: 1261–1271.
16. Bachem, A., S. Güttler, E. Hartung, F. Ebstein, M. Schaefer, A. Tannert, A. Salama, K. Movassaghi, C. Opitz, H. W. Mages, et al. 2010. Superior antigen cross-presentation and XCR1 expression define human CD11c$^+$CD141$^+$ cells as homologues of mouse CD8$^+$ dendritic cells. *J. Exp. Med.* 207: 1273–1281.
17. Haniffa, M., A. Shin, V. Bigley, N. McGovern, P. Teo, P. See, P. S. Wasan, X. N. Wang, F. Malinarich, B. Malleret, et al. 2012. Human tissues contain CD141^{hi} cross-presenting dendritic cells with functional homology to mouse CD103$^+$ nonlymphoid dendritic cells. *Immunity* 37: 60–73.
18. Robbins, S. H., T. Walzer, D. Dembélé, C. Thibault, A. Defays, G. Bessou, H. Xu, E. Vivier, M. Sellars, P. Pierre, et al. 2008. Novel insights into the relationships between dendritic cell subsets in human and mouse revealed by genome-wide expression profiling. *Genome Biol.* 9: R17.
19. Stock, A., S. Booth, and V. Cerundolo. 2011. Prostaglandin E_2 suppresses the differentiation of retinoic acid-producing dendritic cells in mice and humans. *J. Exp. Med.* 208: 761–773.
20. Miyara, M., Y. Yoshioka, A. Kitoh, T. Shima, K. Wing, A. Niwa, C. Parizot, C. Taflin, T. Heike, D. Valeyre, et al. 2009. Functional delineation and differentiation dynamics of human CD4$^+$ T cells expressing the FoxP3 transcription factor. *Immunity* 30: 899–911.
21. Iyoda, T., S. Shimoyama, K. Liu, Y. Omatsu, Y. Akiyama, Y. Maeda, K. Takahara, R. M. Steinman, and K. Inaba. 2002. The CD8$^+$ dendritic cell subset selectively endocytoses dying cells in culture and in vivo. *J. Exp. Med.* 195: 1289–1302.
22. Ito, T., M. Inaba, K. Inaba, J. Toki, S. Sogo, T. Iguchi, Y. Adachi, K. Yamaguchi, R. Amakawa, J. Valladeau, et al. 1999. A CD1a$^+$/CD11c$^+$ subset of human blood dendritic cells is a direct precursor of Langerhans cells. *J. Immunol.* 163: 1409–1419.
23. Penna, G., and L. Adorini. 2000. 1α,25-Dihydroxyvitamin D3 inhibits differentiation, maturation, activation, and survival of dendritic cells leading to impaired alloreactive T cell activation. *J. Immunol.* 164: 2405–2411.
24. Piemonti, L., P. Monti, M. Sironi, P. Fraticelli, B. E. Leone, E. Dal Cin, P. Allavena, and V. Di Carlo. 2000. Vitamin D_3 affects differentiation, maturation, and function of human monocyte-derived dendritic cells. *J. Immunol.* 164: 4443–4451.
25. Penna, G., S. Amuchastegui, N. Giarratana, K. C. Daniel, M. Vulcano, S. Sozzani, and L. Adorini. 2007. 1,25-Dihydroxyvitamin D_3 selectively modulates tolerogenic properties in myeloid but not plasmacytoid dendritic cells. *J. Immunol.* 178: 145–153.
26. Spiegl, N., S. Didichenko, P. McCaffery, H. Langen, and C. A. Dahinden. 2008. Human basophils activated by mast cell-derived IL-3 express retinaldehyde dehydrogenase-II and produce the immunoregulatory mediator retinoic acid. *Blood* 112: 3762–3771.
27. Mora, J. R., M. Iwata, and U. H. von Andrian. 2008. Vitamin effects on the immune system: vitamins A and D take centre stage. *Nat. Rev. Immunol.* 8: 685–698.
28. Barone, F. C., E. A. Irving, A. M. Ray, J. C. Lee, S. Kassis, S. Kumar, A. M. Badger, R. F. White, M. J. McVey, J. J. Legos, et al. 2001. SB 239063, a second-generation p38 mitogen-activated protein kinase inhibitor, reduces brain injury and neurological deficits in cerebral focal ischemia. *J. Pharmacol. Exp. Ther.* 296: 312–321.
29. Davis, M. I., J. P. Hunt, S. Herrgard, P. Ciceri, L. M. Wodicka, G. Pallares, M. Hocker, D. K. Treiber, and P. P. Zarrinkar. 2011. Comprehensive analysis of kinase inhibitor selectivity. *Nat. Biotechnol.* 29: 1046–1051.
30. Mora, J. R., G. Cheng, D. Picarella, M. Briskin, N. Buchanan, and U. H. von Andrian. 2005. Reciprocal and dynamic control of CD8 T cell homing by dendritic cells from skin- and gut-associated lymphoid tissues. *J. Exp. Med.* 201: 303–316.
31. Szatmari, I., A. Pap, R. Rühl, J.-X. Ma, P. A. Illarionov, G. S. Besra, E. Rajnavolgyi, B. Dezso, and L. Nagy. 2006. PPARγ controls CD1d expression by turning on retinoic acid synthesis in developing human dendritic cells. *J. Exp. Med.* 203: 2351–2362.
32. Chang, S.-Y., H.-R. Cha, J.-H. Chang, H.-J. Ko, H. Yang, B. Malissen, M. Iwata, and M.-N. Kweon. 2010. Lack of retinoic acid leads to increased langerin-expressing dendritic cells in gut-associated lymphoid tissues. *Gastroenterology* 138: 1468–1478, e1–e6.
33. Bastie, J. N., N. Balitrand, F. Guidez, I. Guillemot, J. Larghero, C. Calabresse, C. Chomienne, and L. Delva. 2004. 1α,25-Dihydroxyvitamin D3 transrepresses retinoic acid transcriptional activity via vitamin D receptor in myeloid cells. *Mol. Endocrinol.* 18: 2685–2699.
34. Jaensson, E., H. Uronen-Hansson, O. Pabst, B. Eksteen, J. Tian, J. L. Coombes, P.-L. Berg, T. Davidsson, F. Powrie, B. Johansson-Lindbom, and W. W. Agace. 2008. Small intestinal CD103$^+$ dendritic cells display unique functional properties that are conserved between mice and humans. *J. Exp. Med.* 205: 2139–2149.
35. Sigmundsdottir, H., J. Pan, G. F. Debes, C. Alt, A. Habtezion, D. Soler, and E. C. Butcher. 2007. DCs metabolize sunlight-induced vitamin D3 to 'program' T cell attraction to the epidermal chemokine CCL27. *Nat. Immunol.* 8: 285–293.
36. Zehnder, D., R. Bland, M. C. Williams, R. W. McNinch, A. J. Howie, P. M. Stewart, and M. Hewison. 2001. Extrarenal expression of 25-hydroxyvitamin d(3)-1 α-hydroxylase. *J. Clin. Endocrinol. Metab.* 86: 888–894.
37. Hewison, M. 2012. An update on vitamin D and human immunity. *Clin. Endocrinol.* 76: 315–325.
38. Iwata, M., Y. Eshima, and H. Kagechika. 2003. Retinoic acids exert direct effects on T cells to suppress Th1 development and enhance Th2 development via retinoic acid receptors. *Int. Immunol.* 15: 1017–1025.
39. Allen, J. E., and T. A. Wynn. 2011. Evolution of Th2 immunity: a rapid repair response to tissue destructive pathogens. *PLoS Pathog.* 7: e1002003.
40. Palm, N. W., R. K. Rosenstein, and R. Medzhitov. 2012. Allergic host defences. *Nature* 484: 465–472.
41. Chu, C.-C., N. Ali, P. Karagiannis, P. Di Meglio, A. Skowera, L. Napolitano, G. Barinaga, K. Grys, E. Sharif-Paghaleh, S. N. Karagiannis, et al. 2012. Resident CD141 (BDCA3)$^+$ dendritic cells in human skin produce IL-10 and induce regulatory T cells that suppress skin inflammation. *J. Exp. Med.* 209: 935–945.

Virology 449 (2014) 82–87

Contents lists available at ScienceDirect

Virology

journal homepage: www.elsevier.com/locate/yviro

Defining HIV-1 Vif residues that interact with CBFβ by site-directed mutagenesis

Yusuke Matsui [a], Keisuke Shindo [a,*], Kayoko Nagata [a], Katsuhiro Io [a], Kohei Tada [a], Fumie Iwai [a], Masayuki Kobayashi [a], Norimitsu Kadowaki [a], Reuben S. Harris [b,c], Akifumi Takaori-Kondo [a]

[a] Department of Hematology and Oncology, Graduate School of Medicine, Kyoto University, Kyoto 606-8507, Japan
[b] Department of Biochemistry, Molecular Biology and Biophysics, University of Minnesota, MN 55455, United States
[c] Institute for Molecular Virology, University of Minnesota, MN 55455, United States

ARTICLE INFO

Article history:
Received 28 August 2013
Returned to author for revisions
13 September 2013
Accepted 1 November 2013
Available online 26 November 2013

Keywords:
HIV-1
Vif
CBFβ
Interaction
Host factors

ABSTRACT

Vif is essential for HIV-1 replication in T cells and macrophages. Vif recruits a host ubiquitin ligase complex to promote proteasomal degradation of the APOBEC3 restriction factors by poly-ubiquitination. The cellular transcription cofactor CBFβ is required for Vif function by stabilizing the Vif protein and promoting recruitment of a cellular Cullin5-RING ubiquitin ligase complex. Interaction between Vif and CBFβ is a promising therapeutic target, but little is known about the interfacial residues. We now demonstrate that Vif conserved residues E88/W89 are crucial for CBFβ binding. Substitution of E88/W89 to alanines impaired binding to CBFβ, degradation of APOBEC3, and virus infectivity in the presence of APOBEC3 in single-cycle infection. In spreading infection, NL4-3 with Vif E88A/W89A mutation replicated comparably to wild-type virus in permissive CEM-SS cells, but not in multiple APOBEC3 expressing non-permissive CEM cells. These results support a model in which HIV-1 Vif residues E88/W89 may participate in binding CBFβ.

Introduction

HIV-1 Vif is one of six viral accessory proteins and it is essential for the viral replication in T cells and macrophages (Gabuzda et al., 1992, 1994). Vif recruits host proteins, cullin 5 (CUL5), RING-box protein 2 (RBX2), elongin C (ELOC) and elongin B (ELOB), and forms a ubiquitin ligase complex that promotes poly-ubiquitination and proteasomal degradation of the APOBEC3 (A3) retrovirus restriction factors (Jäger et al., 2011; Marin et al., 2003; Sheehy et al., 2003; Shirakawa et al., 2006; Stopak et al., 2003; Yu et al., 2003). A3s are DNA cytosine deaminases that convert cytosines to uracils in single-stranded DNA (Chelico et al., 2006; Harris et al., 2003). In the absence of the Vif protein, at least two A3 family members, A3F and A3G, are efficiently incorporated into budding virions, where they deaminate cytosines in newly reverse-transcribed minus-strand virus DNA in target cells, leading to guanine to adenine hypermutation of the virus genome (Harris et al., 2003; Hultquist et al., 2011b; Sheehy et al., 2002; Zhang et al., 2003).

Amino acid sequences of HIV-1 Vif vary among viral strains, but more than ten regions of residues are conserved (Dang et al., 2010), and several conserved motifs have been shown to interact with host proteins. The BC-box motif ^{144}SLQYLA^{149} binds to ELOC (Mehle et al., 2004; Yu et al., 2004), and the HCCH motif ^{108}Hx$_5$Cx$_{17-18}$Cx$_{3-5}$H^{139} binds to CUL5 (Luo et al., 2005; Mehle et al., 2006). Furthermore, the N-terminal half of Vif contains distinct regions involved in the Vif-A3 protein-protein interactions; ^{11}WQxDRMR^{17} and ^{76}ExxW^{79} motifs are involved in neutralization of A3F (He et al., 2008; Russell and Pathak, 2007), whereas ^{40}YRHHY^{44} motif is involved in neutralization of A3G (Russell and Pathak, 2007); ^{22}KSLVK^{26} and ^{55}VxIPLx4-5Lxφx2YWxL^{72} motifs were reported to be involved in neutralization of both A3F and A3G (Chen et al., 2009; Dang et al., 2009; He et al., 2008; Pery et al., 2009), although there exists a report that K26 is required for neutralization of A3G, but not of A3F (Albin et al., 2010).

Recently, the transcription factor core binding factor-β (CBFβ) has been shown to be involved in the Vif ubiquitin ligase complex (Jäger et al., 2011; Zhang et al., 2011), and critical for its function by stabilizing the Vif protein in cells (Jäger et al., 2011), and enabling the recruitment of CUL5 (Zhang et al., 2011). There are two isoforms of CBFβ, and both isoforms stabilize Vif protein, enhance A3 degradation, and increase virion infectivity (Hultquist et al., 2011a). Thus, the interaction between Vif and CBFβ is a promising

* Correspondence to: Department of Hematology and Oncology, Graduate School of Medicine, 54 Shogoin-Kawaracho, Sakyo-ku, Kyoto, 606-8507 Japan.
Tel: +81 75 751 4964. Fax: +81 75 751 4963.
E-mail address: shind009@kuhp.kyoto-u.ac.jp (K. Shindo).

0042-6822/$ - see front matter © 2013 Elsevier Inc. All rights reserved.
http://dx.doi.org/10.1016/j.virol.2013.11.004

therapeutic target, but little is known about the interfacial amino acids. Hultquist et al. reported that surface F68 residue of CBFβ is involved in binding and stabilizing Vif (Hultquist et al., 2012). Zhang et al. reported that W21 and W38 residues of Vif are required for binding to CBFβ by co-immunoprecipitation experiments (Zhang et al., 2011; Kim et al., 2013). Furthermore, Kim et al. recently suggested that L64 and I66 residues are involved in binding to CBFβ by co-purification in *Escherichia coli* (Kim et al., 2013).

Because a previous study indicated that a hydrophilic region ^{88}EWRKKR^{93} is essential for Vif expression and HIV-1 replication (Fujita et al., 2003), we hypothesized that conserved residues E88 and W89 in this region may be required for CBFβ binding. In this study, we generated amino acid substitution mutants of these residues as well as W21 and W38, and simultaneously analyzed both binding to CBFβ and Vif-mediated degradation of A3F and A3G. We show that the conserved residues E88 and W89 of HIV-1 Vif are directly involved in CBFβ binding and Vif-mediated degradation of A3F and A3G.

Results

The conserved residue W89 of HIV-1 Vif is required for the interaction with CBFβ

To test our hypothesis that conserved residues E88 and W89 may be required for CBFβ binding, we generated nine Vif amino acid substitution mutants, D14A/R15A, W21A, W38A, Y40A, Y69A, G84D, E88A, W89A, and E88A/W89A (Fig. 1A). W21 and W38 were reported to be involved in CBFβ binding (Zhang et al., 2011), D14 and R15 for APOBEC3F binding (Russell and Pathak, 2007), Y40 for A3G binding (Russell and Pathak, 2007), Y69 and G84 for both A3F and A3G binding (Dang et al., 2010; Pery et al., 2009). All of these residues are highly conserved, suggesting that they could be involved in CBFβ binding region of Vif. We first performed co-immunoprecipitation experiments in 293T cells by over-expression of Vif with C-terminal myc tag. Vif is a relatively unstable protein with a short half-life and it is degraded by the cellular proteasome (Dussart et al., 2004; Fujita et al., 2004; Mehle et al., 2004). Mouse double minute 2 homolog (MDM2) is the E3 ubiquitin ligase which targets Vif for degradation (Izumi et al., 2009). Because it has been reported that Vif degradation is accelerated in the absence of CBFβ, and that treatment with the proteasome inhibitor MG132 reverses this effect (Jäger et al., 2011), we used MG132 to minimize proteasomal proteolysis of Vif in cell culture and immunoprecipitation experiments. Although we transfected with the same amount of plasmid DNA, expression levels of E88A, W38A, D14/R15AA, Y40A, Y69A and G84D were comparable to wild-type Vif, but those of W89A, E88/W89A and W21A mutants were obviously impaired (Fig. S1, 2nd top panel). These modest expression levels of these mutants can be simply explained by misfolding, but an alternative explanation is due to loss of CBFβ binding. The amounts of immunoprecipitated Vif protein showed a smaller variation, compared to expression levels (Fig. S1, bottom panel). More importantly, endogenous CBFβ co-precipitated with wild-type Vif, D14A/R15A, Y40A, G84D, and E88A, but not with W21A, W89A, or E88A/W89A (Fig. S1, 3rd top panel). W38A and Y69A showed intermediate results (Fig. S1, lanes 7 and 10, 3rd top panel). To exclude the possibility that low expression of W21A, W89A and E88A/W89A mutants caused the low amount of co-immunoprecipitated CBFβ, we compensated by increasing the amount of transfected plasmid DNA, and performed an additional round of co-immunoprecipitation experiments. Although expression levels of W21A, W89A and E88A/W89A mutants were now higher than wild-type Vif, endogenous CBFβ did not co-precipitate with these mutants (Fig. 1B). We next examined whether CUL5 co-precipitated with Vif mutants by immunoblotting with some of the samples of Fig. 1B, because CBFβ binding has been reported to be required for Vif to interact with CUL5 (Zhang et al., 2011). Endogenous CUL5 appeared to co-precipitate with wild-type Vif, but not with W21A, W38A, W89A, or E88A/W89A (Fig. 1C, 2nd bottom panel). All

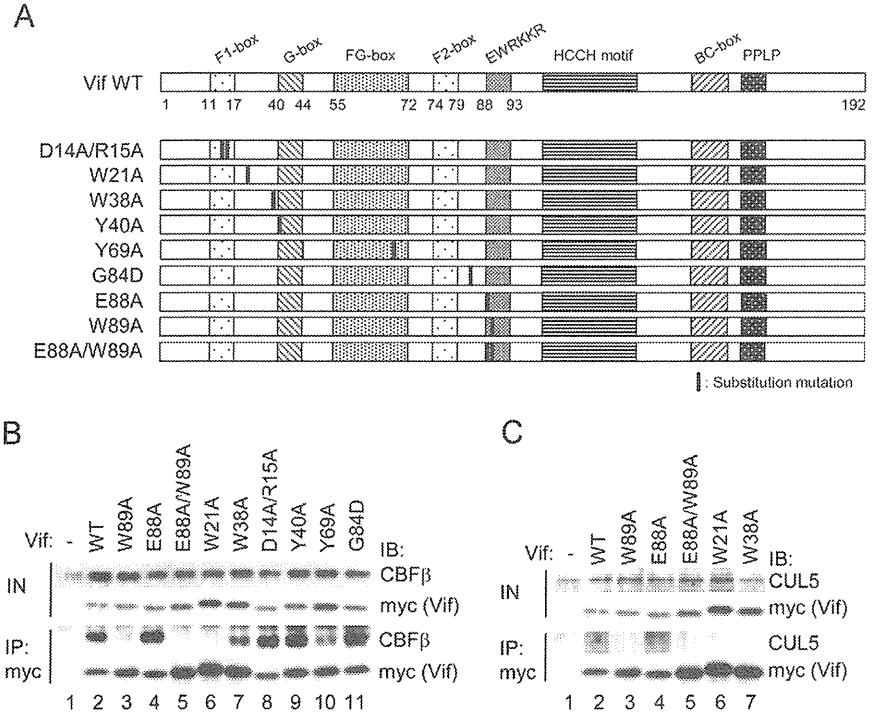

Fig. 1. Vif substitution mutants and binding capacity to CBFβ. (A) Schematic of Vif conserved motifs and nine substitution mutants generated. The residues substituted are indicated by bold lines. (B) Co-immunoprecipitation of endogenous CBFβ with Vif. Lysates of 293T cells transiently expressing myc-tagged Vif wild-type or mutant were immunoprecipitated by anti-myc serum. Samples were analyzed by immunoblotting with anti-CBFβ and anti-myc sera. (C) Co-immunoprecipitation of endogenous CUL5 with Vif. Samples from (B) were also analyzed with anti-CUL5 serum. Panels for Vif were re-produced from (B).

of these mutants of Vif bound to ELOB (Fig. S2), suggesting that they are not entirely misfolded proteins, although previous reports indicated that fragments of the Vif BC box is sufficient for binding to ELOB and ELOC (Bergeron et al., 2010; Wolfe et al., 2010). Altogether, these results suggest that W89 is involved in CBFβ binding, as well as W21 and W38.

The substitution of E88/W89 to alanines impairs Vif-mediated degradation of both A3F and A3G proteins

To examine whether the loss of binding to CBFβ causes impaired Vif-mediated degradation of A3 proteins, we next performed a series of co-transfection and immunoblot experiments. 293T cells were co-transfected with expression vectors for A3G with myc tag and Vif wild-type or mutant, and protein levels of A3G were analyzed by immunoblotting. To obtain comparable expression levels of each of the Vif mutants, we again adjusted the amount of plasmid DNA transfected. Co-transfection of wild-type Vif reduced APOBEC3G levels, but E88A/W89A, W21A or W38A did not (Fig. 2A, lanes 1, 2 and 7–12). E88A or W89A alone reduced A3G levels close to wild-type Vif (Fig. 2A, lanes 3–6). Because W21 and W38 are close to A3G binding residues of Vif, ^{40}YRHHY^{44}, the loss of A3G degradation by W21A or W38A might be caused by loss of A3G binding. To exclude this possibility, we next performed co-transfection experiments with Vif and A3F expression vectors and similar results were obtained (Fig. 2B). These results suggest that the substitution of E88/W89 as well as W21 and W38 to alanines leads to an impairment of Vif-mediated degradation of both A3F and A3G due to the loss of binding to CBFβ, not to A3F or A3G.

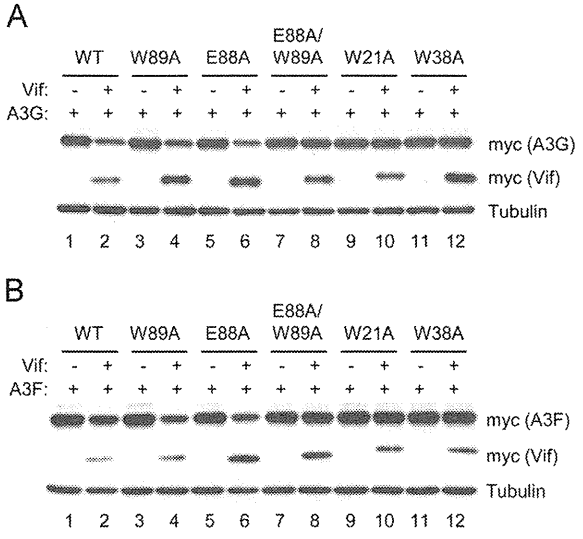

Fig. 2. Degradation of A3F and A3G by Vif. (A) Degradation of A3G. HEK293T cells were co-transfected with expression vectors for myc-tagged A3G and Vif wild-type or mutant, and protein levels of A3G and Vif were analyzed by immunoblotting with anti-myc serum and anti-tubulin antibody for loading control. The same amount of the A3G expression plasmid was transfected in each sample. (B) Degradation of A3F. Similar experiments to (A), but an A3F expression vector was used instead of that of A3G.

The substitution of E88/W89 to alanines impairs the ability of Vif to counteract the restriction by both A3F and A3G

To examine the ability of Vif mutants to counteract the restriction of HIV-1 by A3 proteins, we next performed single cycle infection experiments using luciferase-reporter viruses. The Vif mutations were introduced into pNL4-3 ΔEnv-Luc, and transfected into 293T cells with co-transfection of VSV-G expression plasmid in the presence or absence of co-transfection of A3G expression plasmid. Virus-containing supernatant was harvested and infectivity was measured by challenging to fresh 293T cells and assaying luciferase activity. Viruses with Vif mutations showed comparable infectivity in the absence of A3G, as expected (Fig. 3A). In the presence of A3G, virus with E88A mutation showed comparable infectivity to wild-type, but virus with W21A, W38A or E88A/W89A showed deeply impaired infectivity close to that of ΔVif (Fig. 3A). Virus with W89A showed intermediate and obviously impaired infectivity in the presence of A3G (Fig. 3A). We also performed these assays with A3F instead of A3G, and obtained similar results (Fig. 3B). These data indicate that E88/W89 residues as well as W21 and W38 are involved in Vif activity to counteract both A3F and A3G, suggesting these residues are involved in CBFβ binding, not A3F or A3G binding.

The substitution of E88/W89 to alanines impairs HIV-1 replication in non-permissive CEM cells

Finally, we performed spreading infection experiments in both permissive CEM-SS and multiple A3-expressing CEM cells. We introduced Vif mutations into NL4-3, a replication-competent

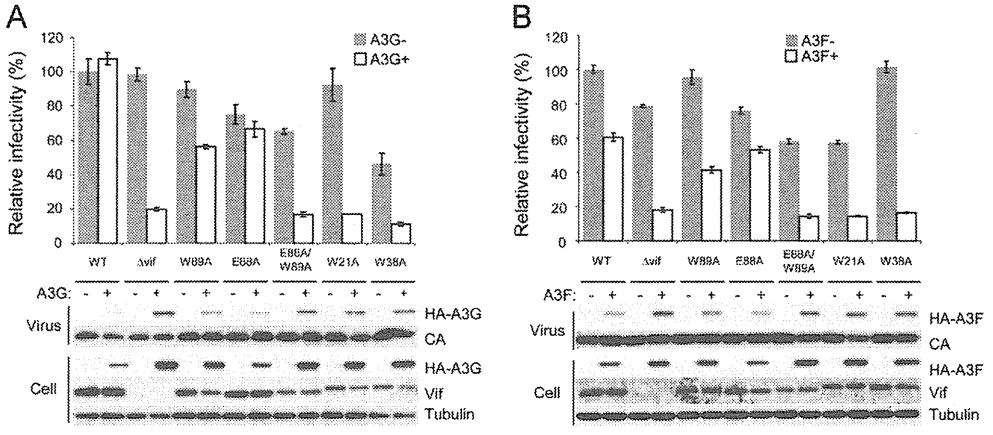

Fig. 3. Single-cycle infection experiments with VSV-G pseudo-typed viruses with vif mutations. (A) Counteracting abilities of Vif mutants against the restriction by A3G. 293T cells were transfected with pNL43/ΔEnv-Luc with vif mutation, together with pVSV-G, in the presence or absence of pcDNA3/HA-A3G. pNL43/ΔEnv-Luc without vif mutation and pNL43/ΔEnvΔvif-Luc were also used for control. Virus-containing supernatant was challenged to fresh 293T cells and infectivity was determined by luminometer. Values were normalized to that of the virus without vif mutation in the absence of A3G. Average and standard errors of 3 independent experiments are shown. Levels of A3G in cells and virions and Vif in cells were also analyzed by immunoblotting. (B) Counteracting abilities of Vif mutants against the restriction by A3F. Similar experiments to (A), but pcDNA3/HA-A3F was used instead of the A3G plasmid.

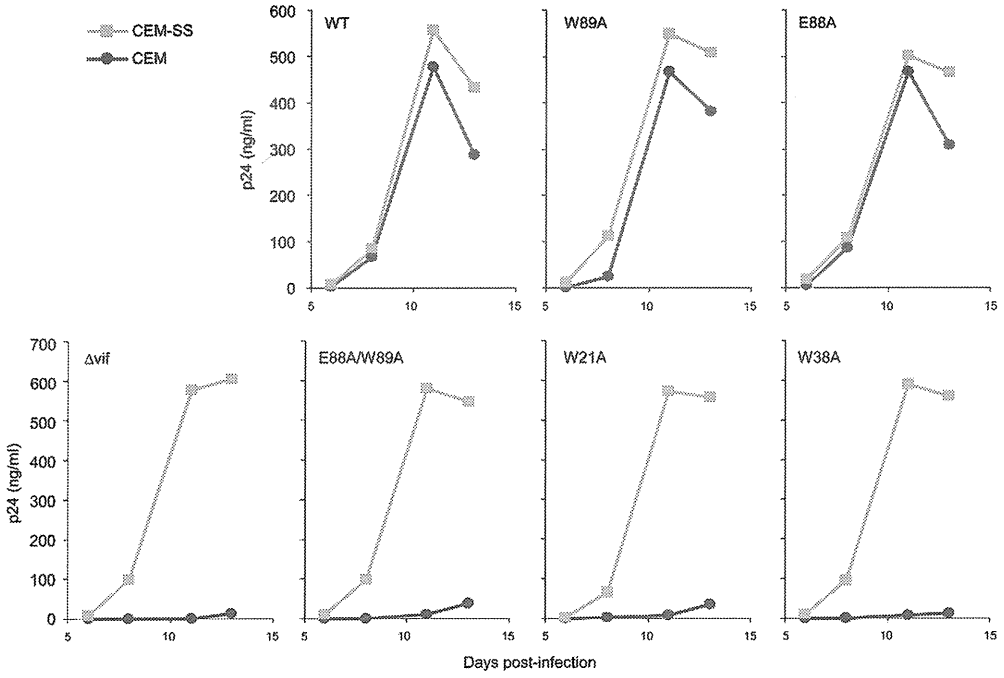

Fig. 4. Spreading infection of NL4-3 with vif mutations. The viruses were produced in 293T cells and challenged to permissive CEM-SS cells and nonpermissive CEM cells at MOI of 0.005. Culture supernatant was collected periodically and p24 levels were determined by ELISA.

molecular clone, and analyzed whether the substitution mutation impairs virus replication with spreading infection assays. Virus with E88A or W89A showed comparable replication profiles to wild-type virus in both CEM-SS and CEM cells. Virus with ΔVif, E88A/W89A, W21A, or W38A showed indistinguishable replication profiles to wild type in CEM-SS cells, as expected, whereas in CEM cells, showed deeply impaired replication profiles (Fig. 4). These results indicate that the residues E88/W89 as well as W21 and W38 are critical for Vif to counteract multiple A3s, suggesting that these residues are directly involved in CBFβ binding.

Discussion

In this study, we report that HIV-1 Vif residues E88 and W89 are involved in CBFβ binding, therefore in rendering Vif capable of stable expression and inducing ubiquitination of both A3F and A3G proteins. Fujita et al. reported that deletion or substitution of these residues impairs steady-state levels of Vif protein and virus replication in nonpermissive H9 cells and monocyte-derived macrophages (Fujita et al., 2003). We confirmed lower expression levels of substitution mutants using both Vif expression vectors and molecular clones of HIV-1. We also confirmed inefficient replication of virus with the mutation using another nonpermissive T cell line, CEM cells. These observations may be all explained by the loss of CBFβ binding.

Our results suggest that the single amino acid substitution mutant W89A does not bind to CBFβ, however this mutant is capable of degradation of A3F and A3G, and supporting replication of the virus in non-permissive CEM cells. This modest conflict may be due to the differences in experimental settings; co-immunoprecipitation experiments test the interactions *in vitro* in complex total cell lysates, and degradation experiments and infectivity experiments test Vif functionality in living cells.

Zhang et al. reported that Vif residues W21 and W38 are involved in binding to CBFβ, but functional correlation of these residues was not described (Zhang et al., 2011). We confirmed that these residues are critical for CBFβ binding, and further demonstrated that these residues are critical for degradation of both A3F and A3G, counteracting restriction by both A3F and A3G, and replication in nonpermissive, multiple A3-expressing cells.

Jäger et al. reported that CBFβ functions to up-regulate steady-state level of Vif protein by using cells with CBFβ knock-down (Jäger et al., 2011). We observed that the levels of Vif mutants that do not bind to CBFβ were obviously lower than that of wild-type Vif. Our observations confirmed and support the Jäger's report by the experiments with different settings.

Several E3 ligases including CUL5, NEDD4, and AIP4, have been reported to induce Vif ubiquitination, although biological implications have not been well defined (Dussart et al., 2004; Mehle et al., 2004). We previously reported that MDM2 targets for Vif as an E3 ligase to induce its ubiquitination and proteasomal degradation, and that the N-terminal region of Vif (residues 4–22) is required for MDM2 binding (Izumi et al., 2009). Because one of the CBFβ binding residues of Vif, W21, is located close to MDM2 binding region, the loss of CBFβ binding might facilitate ubiquitination and degradation of Vif by MDM2. Further investigations will be required to test this possibility.

We provide here the evidence indicating that residues W21, W38, E88 and W89 of HIV-1 Vif are involved in binding surface to CBFβ. Further studies on the Vif-CBFβ co-crystal structure will be the key to understanding Vif-CBFβ interaction surfaces, and to pharmaceutical applications of these pieces of information for patients with HIV-1 infection.

Materials and methods

Plasmid construction

C-terminally myc-tagged Vif expression plasmid, pDON-Vif-myc, was generated by amplifying NL4-3 vif coding sequence with primers ATA GGA TCC ATG GAA AAC AGA TG G CAG GTG GCA GGT GAT G and CGC GTC GAC CTA CAG ATC CTC TTC AGA GAT GAG TTT CTG CTC GTA GTG TCC ATT CAT TGT ATG GCT CCC, and inserting it into pDON-AI (Takara) at BamH I/Sal I sites. Expression plasmids for

Vif mutants were generated by a PCR-based method with properly mutated primers. HA-tagged expression plasmids for A3F and A3G were previously described (Shirakawa et al., 2006). N-terminally myc-tagged expression plasmids for A3F, pcDNA3-myc-A3F, was generated by amplifying coding sequences of human A3F with primers CTA GCT AGC ATG GAG CAG AAA CTC ATC TCT GAA GAG GAT CTG ATG AAG CCT CAC TTC AGA AAC ACA GTG G and GGG GTA CCT CAC TCG AGA ATC TCC TGC AGC TTG CTG, and inserting it into pcDNA3.1 (Invitrogen) at Nhe I/Kpn I sites. C-terminally myc-tagged expression plasmids for A3G, pcDNA3-A3G-myc, was generated by amplifying coding sequences of human A3G with primers ATA CTC GAG AAT GAA GCC TAC TTC AGA AAC ACA GTG and GGG GTA CCC TAC AGA TCC TCT TCA GAG ATG AGT TTC TGC TCG CAG TTT TCC TGA TTC TGG AGA ATG GC, and inserting it into pcDNA3.1 (Invitrogen) at Xho I/Kpn I sites. The luciferase-reporter HIV-1 plasmids for single-cycle infection, pNL43/ΔEnv-Luc and pNL43/ΔEnvΔvif-Luc were previously described (Shindo et al., 2003). Mutations in vif region of pNL43/ΔEnv-Luc and pNL4-3 were introduced by a PCR-based method using internal restriction sites, MSC I at position 4553, and EcoR I at position 5743.

Cell culture and transfection

293T cells were maintained in Dulbecco's modified Eagle's medium supplemented with 10% fetal bovine serum (FBS) and penicillin, streptomycin and glutamine (PSG). CEM and CEM-SS cells were maintained in RPMI1640 medium supplemented with 10% FBS and PSG. 293T cells on 6-well plates were transfected with about 1 μg of plasmid DNA in total using X-tremegene HP DNA transfection reagent (Roche) according to manufacturer's instruction.

Immunoblotting

Primary antibodies for immunoblotting against Vif, A3G and $p24^{Gag}$ were obtained from the NIH AIDS Research and Reference Reagent Program. Rabbit anti-CBFβ serum and mouse anti-Cul5 and anti-HA antibodies were purchased from Santa Cruz. Rabbit anti-myc serum was purchased from Sigma. Mouse anti-tubulin antibody was purchased from Covance. HRP-conjugated secondary antibodies against mouse and rabbit were purchased from GE Healthcare. We used a standard chemiluminescence protocol for immunoblotting with PVDF membrane (Millipore).

Immunoprecipitation

For co-immunoprecipitation to test interaction of Vif mutant to CBFβ, 293T cells were transfected with pDON-Vif-myc or its derivative mutant, treated with MG132 at concentration of 2.5 μM for 16 h, and lysed with co-IP buffer (25 mM HEPES, pH 7.4, 150 mM NaCl, 0.1% Triton X-100, 1 mM EDTA, 1mM $MgCl_2$) supplemented with protease inhibitor cocktail (Nacalai) and MG132. After centrifugation at 20,000 × *g* for 10 min, supernatant was mixed with 2 μg anti-myc rabbit serum (Sigma) for 1 h, and then mixed with 20 μl protein A sepharose (Pharmacia) for 1 h. Beads were washed with co-IP buffer 3 times, and bound protein was eluted with 1 x SDS sample buffer. Samples were analyzed by immunoblotting as described above.

Single-cycle infection

Luciferase encoding HIV-1 particles were produced by transiently transfecting 293T cells at 50% confluency using 0.8 μg pNL43/ΔEnv-Luc or derivative mutant, 0.2 μg pVSV-G and 0.02 μg pcDNA3/HA-A3F, pcDNA3/HA-A3G, or empty vector. After 48 h, virus-containing supernatants were harvested through PVDF filter with 0.45 μm pores (Millipore), and challenged to fresh 293T cells. After 48 h, cells were lysed with Passive lysis buffer (Promega) and luciferase activity was determined by luminometer (2030 Arvo X, Perkin Elmer) using Luciferase Assay System (Promega). Sample preparation of producer cells and virus for immunoblotting was performed as described (Haché et al., 2008).

Spreading infection

293T cells were transfected with NL4-3 molecular clone or derivative mutant, and virus-containing supernatant was harvested through PVDF filters with 0.45 μm pores (Millipore) after 2-day incubation. CEM-SS and CEM cells were inoculated with the supernatant at MOI of 0.005. The culture supernatants were harvested periodically, and analyzed for p24 by an HIV-1 p24 antigen ELISA kit (Zeptometrix).

Acknowledgments

We thank Dr. Y. Koyanagi for BL3 laboratory, Drs. J. Hultquist and A. Land in University of Minnesota for helpful discussion. The following materials were obtained through the AIDS Research and Reference Reagent Program, NIH: rabbit anti-Vif serum 2221 from Dr. Dana Gabuzda, anti-p24 Gag monoclonal antibody 6457 from Dr. Michael H. Malim, and rabbit anti-A3G serum 10201 from Dr. Jaisri Lingappa.

This study was partly supported by Grants-in-aid from the Ministry of Education, Culture, Sports, Science and Technology and from the Ministry of Health, Labor and Welfare in Japan. Work in the Harris lab was supported in part by grants from the National Institutes of Health (R01 AI064046 and P01 GM091743).

Appendix A. Supplementary material

Supplementary data associated with this article can be found in the online version at http://dx.doi.org/10.1016/j.virol.2013.11.004.

References

Albin, J.S., Haché, G., Hultquist, J.F., Brown, W.L., Harris, R.S., 2010. Long-term restriction by APOBEC3F selects human immunodeficiency virus type 1 variants with restored Vif function. J. Virol. 84 (19), 10209–10219.

Bergeron, J.R., Huthoff, H., Veselkov, D.A., Beavil, R.L., Simpson, P.J., Matthews, S.J., Malim, M.H., Sanderson, M.R., 2010. The SOCS-box of HIV-1 Vif interacts with ElonginBC by induced-folding to recruit its Cul5-containing ubiquitin ligase complex. PLoS Pathog 6 (6), e1000925.

Chelico, L., Pham, P., Calabrese, P., Goodman, M.F., 2006. APOBEC3G DNA deaminase acts processively 3′→5′ on single-stranded DNA. Nat. Struct. Mol. Biol. 13 (5), 392–399.

Chen, G., He, Z., Wang, T., Xu, R., Yu, X.F., 2009. A patch of positively charged amino acids surrounding the human immunodeficiency virus type 1 Vif SLVx4Yx9Y motif influences its interaction with APOBEC3G. J. Virol. 83 (17), 8674–8682.

Dang, Y., Davis, R.W., York, I.A., Zheng, Y.H., 2010. Identification of 81LGxGxxIxW89 and 171EDRW174 domains from human immunodeficiency virus type 1 Vif that regulate APOBEC3G and APOBEC3F neutralizing activity. J. Virol. 84 (11), 5741–5750.

Dang, Y., Wang, X., Zhou, T., York, I.A., Zheng, Y.H., 2009. Identification of a novel WxSLVK motif in the N terminus of human immunodeficiency virus and simian immunodeficiency virus Vif that is critical for APOBEC3G and APOBEC3F neutralization. J. Virol. 83 (17), 8544–8552.

Dussart, S., Courcoul, M., Bessou, G., Douaisi, M., Duverger, Y., Vigne, R., Decroly, E., 2004. The Vif protein of human immunodeficiency virus type 1 is posttranslationally modified by ubiquitin. Biochem. Biophys. Res. Commun. 315 (1), 66–72.

Fujita, M., Akari, H., Sakurai, A., Yoshida, A., Chiba, T., Tanaka, K., Strebel, K., Adachi, A., 2004. Expression of HIV-1 accessory protein Vif is controlled uniquely to be low and optimal by proteasome degradation. Microb. Infect. 6 (9), 791–798.

Fujita, M., Sakurai, A., Yoshida, A., Miyaura, M., Koyama, A.H., Sakai, K., Adachi, A., 2003. Amino acid residues 88 and 89 in the central hydrophilic region of human immunodeficiency virus type 1 Vif are critical for viral infectivity by enhancing the steady-state expression of Vif. J. Virol. 77 (2), 1626–1632.

Gabuzda, D.H., Lawrence, K., Langhoff, E., Terwilliger, E., Dorfman, T., Haseltine, W.A., Sodroski, J., 1992. Role of vif in replication of human immunodeficiency virus type 1 in CD4+ T lymphocytes. J. Virol. 66 (11), 6489–6495.

Gabuzda, D.H., Li, H., Lawrence, K., Vasir, B.S., Crawford, K., Langhoff, E., 1994. Essential role of vif in establishing productive HIV-1 infection in peripheral

blood T lymphocytes and monocyte/macrophages. J. Acquir. Immune Defic. Syndr. 7 (9), 908–915.
Haché, G., Shindo, K., Albin, J.S., Harris, R.S., 2008. Evolution of HIV-1 isolates that use a novel Vif-independent mechanism to resist restriction by human APOBEC3G. Curr. Biol. 18 (11), 819–824.
Harris, R.S., Bishop, K.N., Sheehy, A.M., Craig, H.M., Petersen-Mahrt, S.K., Watt, I.N., Neuberger, M.S., Malim, M.H., 2003. DNA deamination mediates innate immunity to retroviral infection. Cell 113 (6), 803–809.
He, Z., Zhang, W., Chen, G., Xu, R., Yu, X.F., 2008. Characterization of conserved motifs in HIV-1 Vif required for APOBEC3G and APOBEC3F interaction. J. Mol. Biol. 381 (4), 1000–1011.
Hultquist, J.F., Binka, M., LaRue, R.S., Simon, V., Harris, R.S., 2011a. Vif proteins of human and simian immunodeficiency viruses require cellular CBFbeta to degrade APOBEC3 restriction factors. J. Virol. 86 (5), 2874–2877.
Hultquist, J.F., Lengyel, J.A., Refsland, E.W., LaRue, R.S., Lackey, L., Brown, W.L., Harris, R.S., 2011b. Human and rhesus APOBEC3D, APOBEC3F, APOBEC3G, and APOBEC3H demonstrate a conserved capacity to restrict Vif-deficient HIV-1. J. Virol. 85 (21), 11220–11234.
Hultquist, J.F., McDougle, R.M., Anderson, B.D., Harris, R.S., 2012. HIV type 1 viral infectivity factor and the RUNX transcription factors interact with core binding factor beta on genetically distinct surfaces. AIDS Res. Hum. Retroviruses 28 (12), 1543–1551.
Izumi, T., Takaori-Kondo, A., Shirakawa, K., Higashitsuji, H., Itoh, K., Io, K., Matsui, M., Iwai, K., Kondoh, H., Sato, T., Tomonaga, M., Ikeda, S., Akari, H., Koyanagi, Y., Fujita, J., Uchiyama, T., 2009. MDM2 is a novel E3 ligase for HIV-1 Vif. Retrovirology 6, 1.
Jäger, S., Kim, D.Y., Hultquist, J.F., Shindo, K., LaRue, R.S., Kwon, E., Li, M., Anderson, B.D., Yen, L., Stanley, D., Mahon, C., Kane, J., Franks-Skiba, K., Cimermancic, P., Burlingame, A., Sali, A., Craik, C.S., Harris, R.S., Gross, J.D., Krogan, N.J., 2011. Vif hijacks CBF-beta to degrade APOBEC3G and promote HIV-1 infection. Nature 481 (7381), 371–375.
Kim, D.Y., Kwon, E., Hartley, P.D., Crosby, D.C., Mann, S., Krogan, N.J., Gross, J.D., 2013. CBFbeta stabilizes HIV Vif to counteract APOBEC3 at the expense of RUNX1 target gene expression. Mol. Cell 49 (4), 632–644.
Luo, K., Xiao, Z., Ehrlich, E., Yu, Y., Liu, B., Zheng, S., Yu, X.F., 2005. Primate lentiviral virion infectivity factors are substrate receptors that assemble with cullin 5-E3 ligase through a HCCH motif to suppress APOBEC3G. Proc. Nat. Acad. Sci. U.S.A. 102 (32), 11444–11449.
Marin, M., Rose, K.M., Kozak, S.L., Kabat, D., 2003. HIV-1 Vif protein binds the editing enzyme APOBEC3G and induces its degradation. Nat. Med. 9 (11), 1398–1403.
Mehle, A., Goncalves, J., Santa-Marta, M., McPike, M., Gabuzda, D., 2004. Phosphorylation of a novel SOCS-box regulates assembly of the HIV-1 Vif-Cul5 complex that promotes APOBEC3G degradation. Genes Dev. 18 (23), 2861–2866.
Mehle, A., Thomas, E.R., Rajendran, K.S., Gabuzda, D., 2006. A zinc-binding region in Vif binds Cul5 and determines cullin selection. J. Biol. Chem. 281 (25), 17259–17265.
Pery, E., Rajendran, K.S., Brazier, A.J., Gabuzda, D., 2009. Regulation of APOBEC3 proteins by a novel YXXL motif in human immunodeficiency virus type 1 Vif and simian immunodeficiency virus SIVagm Vif. J. Virol. 83 (5), 2374–2381.
Russell, R.A., Pathak, V.K., 2007. Identification of two distinct human immunodeficiency virus type 1 Vif determinants critical for interactions with human APOBEC3G and APOBEC3F. J. Virol. 81 (15), 8201–8210.
Sheehy, A.M., Gaddis, N.C., Choi, J.D., Malim, M.H., 2002. Isolation of a human gene that inhibits HIV-1 infection and is suppressed by the viral Vif protein. Nature 418 (6898), 646–650.
Sheehy, A.M., Gaddis, N.C., Malim, M.H., 2003. The antiretroviral enzyme APOBEC3G is degraded by the proteasome in response to HIV-1 Vif. Nat. Med. 9 (11), 1404–1407.
Shindo, K., Takaori-Kondo, A., Kobayashi, M., Abudu, A., Fukunaga, K., Uchiyama, T., 2003. The enzymatic activity of CEM15/Apobec-3G is essential for the regulation of the infectivity of HIV-1 virion but not a sole determinant of its antiviral activity. J. Biol. Chem. 278 (45), 44412–44416.
Shirakawa, K., Takaori-Kondo, A., Kobayashi, M., Tomonaga, M., Izumi, T., Fukunaga, K., Sasada, A., Abudu, A., Miyauchi, Y., Akari, H., Iwai, K., Uchiyama, T., 2006. Ubiquitination of APOBEC3 proteins by the Vif-Cullin5-ElonginB-ElonginC complex. Virology 344 (2), 263–266.
Stopak, K., de Noronha, C., Yonemoto, W., Greene, W.C., 2003. HIV-1 Vif blocks the antiviral activity of APOBEC3G by impairing both its translation and intracellular stability. Mol. Cell 12 (3), 591–601.
Wolfe, L.S., Stanley, B.J., Liu, C., Eliason, W.K., Xiong, Y., 2010. Dissection of the HIV Vif interaction with human E3 ubiquitin ligase. J Virol 84 (14), 7135–7139.
Yu, X., Yu, Y., Liu, B., Luo, K., Kong, W., Mao, P., Yu, X.F., 2003. Induction of APOBEC3G ubiquitination and degradation by an HIV-1 Vif-Cul5-SCF complex. Science 302 (5647), 1056–1060.
Yu, Y., Xiao, Z., Ehrlich, E.S., Yu, X., Yu, X.F., 2004. Selective assembly of HIV-1 Vif-Cul5-ElonginB-ElonginC E3 ubiquitin ligase complex through a novel SOCS box and upstream cysteines. Genes Dev. 18 (23), 2867–2872.
Zhang, H., Yang, B., Pomerantz, R.J., Zhang, C., Arunachalam, S.C., Gao, L., 2003. The cytidine deaminase CEM15 induces hypermutation in newly synthesized HIV-1 DNA. Nature 424 (6944), 94–98.
Zhang, W., Du, J., Evans, S.L., Yu, Y., Yu, X.F., 2011. T-cell differentiation factor CBF-beta regulates HIV-1 Vif-mediated evasion of host restriction. Nature 481 (7381), 376–379.